Heliyon 10 (2024) e36909

Contents lists available at ScienceDirect

Heliyon

journal homepage: www.cell.com/heliyon

Research article

LC-MS based strategy for chemical profiling and quantification of dispensing granules of *Ginkgo biloba* seeds

Facheng Zhang [a,1], Qingqing Fei [b,c,1], Xiaojun Huang [b,c], Sheng Yu [b,c], Rongli Qiu [b,c], Lan Guan [a], Baoxiang Wu [a], Mingqiu Shan [b,c,*]

[a] *Polifarma (Nanjing) Co., Ltd., Nanjing, 210038, PR China*
[b] *Jiangsu Collaborative Innovation Center of Chinese Medicinal Resources Industrialization, Nanjing University of Chinese Medicine, Nanjing, 210023, PR China*
[c] *School of Pharmacy, Nanjing University of Chinese Medicine, Nanjing, 210023, PR China*

ARTICLE INFO

Keywords:
Dispensing granules of *Ginkgo biloba* seeds
LC-MS
Qualitative analysis
Quantitative analysis

ABSTRACT

Ginkgo biloba seeds have been used as a traditional Chinese medicine for hundreds of years to treat diseases such as cervicitis, cough, asthma and other lung diseases. As a novel form, the dispensing granules (GSDG) of *Ginkgo biloba* seeds have been widely employed in clinic. However, its chemical profiling is not yet clear, which has restricted in-depth research in many fields.

In this study, a high performance liquid chromatography coupled with quardrupole time-of-flight mass spectrometry method was used for the component characteration with the help of accurate molecular weights, fragmentation pathways, reported data, literatures and even some reference standards. Furthermore, in multiple-reaction monitoring mode, a high performance liquid chromatography coupled with quadrupole linear ion trap mass spectrometry method was developed and applied for simultaneous determination of the bioactive phytochemicals.

As a result, a total of 56 components in GSDG were identified including 12 amino acids, 9 organic acids, 6 nucleosides and nucleobases, 6 flavonoids, 5 vitamins, 5 terpenoid lactones, 4 carbohydrates and 9 other compounds As for quantitative analysis, glutamic acid, asparatic acid, histidine, ginkgolide A, ginkgolide B, ginkgolide C, ginkgolide J, eucomic acid, *N*-(*N*-glucopyranosyl)-indoleacetylaspartate and *N*-(*N*-glucopyranosyl)-indoleacetylglutamate were selected as the analytes for quanlity marker of GSDG. After necessary validation tests, the developed quantitative method was successfully put into use for 10 batches of GSDG. In all batches, *N*-(*N*-glucopyranosyl)-indoleacetylaspartate was the richest phytochemical with the amount of 17.3–25.7 mg/g while ginkgolide J (0.0197–0.0335 mg/g) was determined to be the poorest.

The study is supposed to exhibit a comprehensive chemical profiling and to provide some strong basis for preparation technology, quality control and even for action mechanism of GSDG, this novel form of Chinese medicine.

* Corresponding author. Jiangsu Collaborative Innovation Center of Chinese Medicinal Resources Industrialization, Nanjing University of Chinese Medicine, Nanjing, 210023, PR China.
E-mail addresses: zhangfc@polifarma.com.cn (F. Zhang), zingfei@163.com (Q. Fei), shanmingqiu@njucm.edu.cn (M. Shan).
[1] Equal first authors.

https://doi.org/10.1016/j.heliyon.2024.e36909
Received 17 June 2024; Received in revised form 22 August 2024; Accepted 23 August 2024
Available online 29 August 2024

1. Introduction

It is well known that the decoction is one of the significant and common dosage forms of Chinese medicines. Clinically, a decoction preparation for administration is usually prepared by patients themselves by boiling all composition drugs as prescribed by doctors with water and then removing the dregs. However, due to lack of standardized procedures and specifications, such as regarding the frequency of decoction (twice or thrice), the decocting process seems to be time-consuming and difficult to provide a stable quality.

In recent decades, dispensing granules (DG), a novel dosage form of Chinese medicines, has been popularly accepted and used [1–3]. The DG is prepared from traditional decoction pieces as the raw material, which involves many technology procedures, including cleaning, washing, cutting, boiling, concentration, drying, granulation and packing [4]. Because of the use of water as the decocting solvent, many water-soluble substances are retained in DG, which means that several drugs can be mixed in DG form and dissolved in hot water, thus quickly and conveniently producing a target decoction. It is acknowledged that the DG has a stable quality relative to the traditional decoction and allows pharmacists to make up a prescription easily and patients to take conveniently. In our opinions, the DG is consistent with the theory of traditional Chinese medicine (TCM) and very near to traditional decoction with thousands of years of history.The DG has been gradually widely used in clinic and focused from researchers in China.

Ginkgo biloba seeds (GS), a famous traditional Chinese medicine, was firstly recorded in *Compendium of Materia Medica* by Li Shizhen in the Ming dynasty [5]. From then on, it has been used for treating phlegm, cough and asthma, vaginal discharge, and frequent enuresis and urination by exerting the effects of warming lung and supplementing qi, calming asthma, stopping tourniquet and urination [6,7]. Nowadays, it is still clinically used to treat asthma, pulmonary tuberculosis, vaginitis, and other conditions [8,9]. The DG form of GS (GSDG) has also been widely employed alone or in combination and has attracted increasing attention. However, similar to the majority of Chinese medicines, the complicated chemical composition of GSDG is still unclear and no publication is available on its full-scale qualitative and quantitative analysis. In many provinces in China, only ginkgolide B or ginkgolide C is included as the quality marker in the local GSDG's quality standard, which does not conform to the concept of "multi-component, multi-pathway, multi-target, multi-effect". This has greatly limited further research work, especially in exploring its substantial basis and action mechanism.

In this study, we used high performance liquid chromatography coupled with quadrupole time-of-flight mass spectrometry (HPLC-QTOF-MS) to characterize GSDG's complex and diverse chemical composition based on the observed retention times, high-resolution MS data, fragmentation pathways in the negative or positive ion mode, combined with related literature and available reference standards. In addition, a high performance liquid chromatography coupled with quadrupole linear ion trap mass spectrometry (HPLC-QTRAP-MS) was established for simultaneous assay of 10 major active phytochemicals in multiple-reaction monitoring (MRM) mode and was successfully applied for 10 batches of GSDG. To our knowledge, the present study is the first to qualitatively analyze GSDG and simultaneously determine multiple bioactive phytochemicals and it is expected to exhibit an integrated chemical profiling of GSDG, and help explore the material basis of this Chinese medicine for its further clinical therapy.

2. Methods

2.1. Materials and reagents

In the present study, both acetonitrile and methanol were of LC-MS grade and bought from Merck (Merck, Darmstadt, Germany), and formic acid (HPLC grade) was bought from Anaqua Chemicals Supply (ACS, Houston, USA). A Milli-Q system (Millipore, Bedford, MA, USA) was used to prepare ultrapure water.

The reference standards of glutamic acid (98.6 %), asparatic acid (99.3 %) and histidine (98.7 %) were provided by Shanghai Macklin Biochemical Technology Co., Ltd. The reference standards of ginkgolide A (98.0 %), ginkgolide B (99.4 %), ginkgolide C (99.0 %), and ginkgolide J (98.2 %) were purchased from Taizhou Dan Ding Biological Technology Co., Ltd. The reference standards of eucomic acid (98.5 %), *N*-(*N*-glucopyranosyl)-indoleacetylaspartate (98.6 %) and *N*-(*N*-glucopyranosyl)-indoleacetylglutamate (98.3 %) were prepared and isolated from GS in our laboratory. The purities of these standards were all determined by HPLC in our laboratory.

10 batches of GSDG (S1-S10) were made and provided by Polifarma (Nanjing) Co., Ltd.

2.2. Preparation standard and sample solutions

2.2.1. Preparation of standard solutions

For the 10 bioactive components, the individual standard solutions were prepared in 50 % methanol. An appropriate volume of each standard solution was added in a 50 mL volumetric flask and diluted with 50 % methanol to obtain the mixed stock standard solution containing 10 analytes as follows: aspartic acid at 4.10 μg/mL, glutamic acid at 3.96 μg/mL, histidine at 4.06 μg/mL, ginkgolide A at 1.09 μg/mL, ginkgolide B at 0.667 μg/mL, ginkgolide C at 0.520 μg/mL, ginkgolide J at 5.15 μg/mL, *N*-(*N*-glucopyranosyl)-indoleacetylaspartate at 99.9 μg/mL, *N*-(*N*-glucopyranosyl)-indoleacetylglutamate at 40.1 μg/mL, and eucomic acid at 19.9 μg/mL. All solutions were stored in a refrigerator at 4 °C and centrifuged at 10000 rpm for 5 min before injection.

2.2.2. Preparation of test solution

0.2 g of GSDG powder was accurately weighed and sonicated for 1h in 40 mL of 50 % methanol. The extract was replenished with 50 % methanol for loss and filtered through a 0.22 μm membrane. Then, the resulting GSDG test solution was treated as the above

standard solutions.

2.3. Qualitative analysis

A Shimadzu HPLC system (Kyoto, Japan) coupled with an AB SCIEX QTOF 5600 mass spectrometer (Foster City, CA, USA) was used for component characterization. With its temperature at 30 °C, A Welch Ultimate AQ-C_{18} column (250 mm × 4.6 mm × 5 μm) was used for chromatographic separation. At the flow rate of 1.0 mL/min, the mobile phase was composed of acetonitrile (A) and 0.3 % formic acid (B) with the elution gradient: 0–5 min, 10 % A; 5–15 min, 10–14 % A; 15–20 min, 14 % A; 20–30 min, 14–25 % A; 30–35 min, 25–35 % A; 35–40 min, 35–85 % A; 40–45min, 85–10 % A. The injection volume was 10 μL. Electron spray ionization (ESI) was employed in the full scan mode with the range of *m/z* 50–1500. Information-dependent acquisition of ions was performed in both negative mode and positive mode with ion spray voltages set at −4500 V and 5500 V, respectively. Other mass parameters were set as follows: curtain gas at 40 psi, both ion source gas 1 and 2 at 60 psi, and ESI temperature at 600 °C.

2.4. Quantitative analysis

For simultaneous assay of the representative phytochemicals, an AB SCIEX QTRAP 5500 mass spectrometer (Foster City, CA, USA) was employed accompanying with a Shimadzu HPLC system (Kyoto, Japan). All 10 analytes were quantified in MRM mode. The Applied Biosystems/MDS Sciex Analyst software (version 1.5.2) was used to design and optimize compound-dependent mass parameters, shown in Table 1. Except the gradient elution program, the chromatographic separation was accomplished in the same conditions as the above in "2.3. Qualitative analysis" including the column and its temperature, flow rate, mobile phase system and injection volume. The gradient elution program was as follow: 0–5 min, 10 % A; 5–7min 10–14 % A; 7–8 min, 14 % A; 8–10 min, 14–25 % A; 10–13 min, 25–35 % A; 13–18 min, 35–85 % A; 18–20 min, 85–95 % A; 20–35min, 95 % A; 35–38 min, 95–10 % A.

2.5. Quantitative method validation

To confirm the applicability of the quantitative method, validation investigation was performed by assessing linearity, LOQ and LOD, repeatability, precision, stability, and recovery.

In the linearity test, a series of standard solutions of at different dilutions (1, 1/2, 1/4, 1/8, 1/16, 1/32, and 1/64) were used to plot the calibration curves with their concentrations (X, μg/mL) and the corresponding peak areas (Y). The S1 sample solution was consecutively analyzed six times in the precision test and was then analyzed at 0, 1, 2, 4, 6, and 8 h in the stability test. Six sample solutions of S1 were quantified for the contents of the target compounds in the repeatability test. In addition, in the recovery test, the reference standard of each analyte was spiked into the S1 sample at 100 % of its amount in the S1 sample to prepare the sample solution in six copies and to calculate the recovery using the following formula: (determined amount−theoretical amount) × 100 %/spiked amount.

3. Result and discussion

3.1. Qualitative analysis

A GS chemical composition database was established on the basis of previous relevant studies. The chemical profiling analysis of GSDG was performed with the Peakview software using the data obtained from HPLC-QTOF-MS, including the exact molecular mass, retention time and other MS/MS data. The determination of chemical formula was based on the common quasi-molecular ion ($[M+H]^+$ or $[M-H]^-$) in the positive or negative mode, with a mass deviation ≤10 ppm. The structural identification was mainly based on MS/MS fragment ions and proposed cleavage pathways in conjunction with the available literature data, and where applicable, confirmed against with the available reference standards. A total of 56 compounds, which were classified into amino acids,

Table 1
MS parameters of the 10 analytes.

Analyte	Formula	Precursor ion (*m/z*)	Product ion (*m/z*)	Declustering potential (V)	Collision energy (eV)	Collision cell exit potential (eV)
Histidine	$C_6H_9N_3O_2$	156.1	110.0	59	10	14
Aspartic acid	$C_4H_7NO_4$	134.1	88.0	59	10	14
Glutamic acid	$C_5H_9NO_4$	148.1	83.9	58	14	14
N-(*N*-glucopyranosyl)-indoleacetylaspartate	$C_{20}H_{24}N_2O_{10}$	451.0	173.0	−80	−38	−15
N-(*N*-glucopyranosyl)-indoleacetylglutamate	$C_{21}H_{26}N_2O_{10}$	465.0	128.1	−140	−36	−9
Eucomic acid	$C_{11}H_{12}O_6$	239.0	178.6	−85	−20	−13
Ginkgolide J	$C_{20}H_{24}O_{10}$	469.2	423.1	−38	−19	−15
Ginkgolide C	$C_{20}H_{24}O_{11}$	439.1	383.3	−150	−21	−15
Ginkgolide B	$C_{20}H_{24}O_{10}$	423.1	367.3	−150	−20	−15
Ginkgolide A	$C_{20}H_{24}O_9$	407.1	351.1	−150	−19	−15

organic acids, nucleobases and nucleosides, flavonoids, vitamins, terpenoid lactones, carbohydrates and other chemical classes, were identified. The total ion chromatograms (TICs) of GSDG are shown in Fig. 1 (A, in the positive and B, in the negative mode). The results of the structure identification for all compounds are listed in Table 2.

3.1.1. Amino acids

A total of 12 amino acids were identified in GSDG in the positive mode, the more favorable ionization mode than the negative mode for this class of phytochemicals. The characteristic loss of a NH_3 (17 Da) or a HCOOH (46 Da) and the loss of a H_2O (18 Da) from the hydroxyl group at the branch chain of the molecules were common in their full scan positive MS/MS spectra. Considering their accurate masses and similar fragmentation pattern, C2 ($C_5H_9NO_2$), C11 ($C_5H_{11}NO_2$) and C32 ($C_4H_7NO_4$) were identified to be proline, valine and aspartic acid, respectively [10–12]. C18 and C19 were found to have almost identical protonated ions and fragment ions, indicating a common chemical formula ($C_6H_{13}NO_2$) and the same breaking pattern. However, a much higher relative intensity was observed for the product ion of $[M+H-HCOOH-NH_3]^+$ of C19 (*m/z* 69.0739) than that of C18 (*m/z* 69.0738). In accordance with their fragment mechanism involving intermediary ion/neutral complexes, C18 and C19 were identified as leucine and isoleucine, respectively [13,14].

C1 showed a quasi-molecular ion $[M+H]^+$ at *m/z* 175.1189, consistent with a molecular formula of $C_6H_{14}N_4O_2$. From this precursor ion, two fragment ions at *m/z* 116.0723 ($C_5H_9NO_2$) and 60.0620 (CH_5N_3) were generated due to the losses of a $NH{=}C(NH_2)_2$ group and a $CH_2{=}CHCH_2CHNH_2COOH$ group, respectively. The first fragment ion further lost a HCOOH unit to produce the base peak ion at *m/z* 70.0703. The product ions at *m/z* 158.0925 $[M+H-NH_3]^+$ and 130.0086 $[M+H-NH_3-CO]^+$ arose from another fragmentation pathway of $[M+H]^+$, i.e., the sequential losses of a NH_3 moiety and a CO unit (28 Da). Based on the observed cleavage behaviors, C1 was identified to be arginine [15].

C21 showed its quasi-molecular ion $[M+H]^+$ at *m/z* 182.0759, consistent with a molecular formula of $C_9H_{11}NO_3$. The calculated degree of unsaturation of 5, supported the presence of a phenyl group in the molecule. The loss of a HCOOH moiety from $[M+H]^+$ produced a product ion at *m/z* 136.0798, which further lost a NH_3 unit to give $[M+H-HCOOH-NH_3]^+$ at *m/z* 119.0534. In addition, $[M+H-HCOOH]^+$ underwent the sequential losses of a $CH_2{=}NH$ moiety and an oxygen atom followed by the rearrangement, resulting in a fragment ion at *m/z* 91.0572, which further produced a product ion $[M+H-HCOOH-CH_2{=}NH-O-CH_2]^+$ at *m/z* 77.0407 by losing a CH_2 group. C25 exhibited similar fragmentation pattern. In its MS/MS spectrum, the protonated ion, decarboxylation ion, and deamination ion were observed at *m/z* 166.0926 ($[M+H]^+$), 120.0830 ($[M+H-HCOOH]^+$), and 103.0571 ($[M+H-HCOOH-NH_3]^+$), respectively, each with a mass difference of 16 Da (O) from the corresponding ion of C21. Furthermore, additional two fragment ions were detected at *m/z* 91.0579 and 77.0434, similar to those of C21. Thus, C21 and C25 were identified to be tyrosine and phenylalanine, respectively [16,17].

The molecular formulas of C5 and C6 were determined to be $C_5H_7NO_3$ and $C_5H_9NO_4$, respectively, based on their protonated ions $[M+H]^+$ at *m/z* 130.0514 and 148.0613, respectively. A difference of H_2O between C5 and C6 indicated that C5 was the dehydration product of C6. In the MS/MS spectrum of C6 (Supplementary Fig. 1), another dehydration (between the amino group and the remote hydroxyl group) was observed, resulting in a product ion at *m/z* 130.0517 $[M+H-H_2O]^+$, which further underwent cleavages via two possible pathways. The first involved the elimination of a CO group, producing a fragment ion at *m/z* 102.0580 $[M+H-H_2O-CO]^+$, followed by the further elimination of a NH_3 moiety, forming another fragment ion at *m/z* 85.0318 $[M+H-H_2O-CO-NH_3]^+$. The

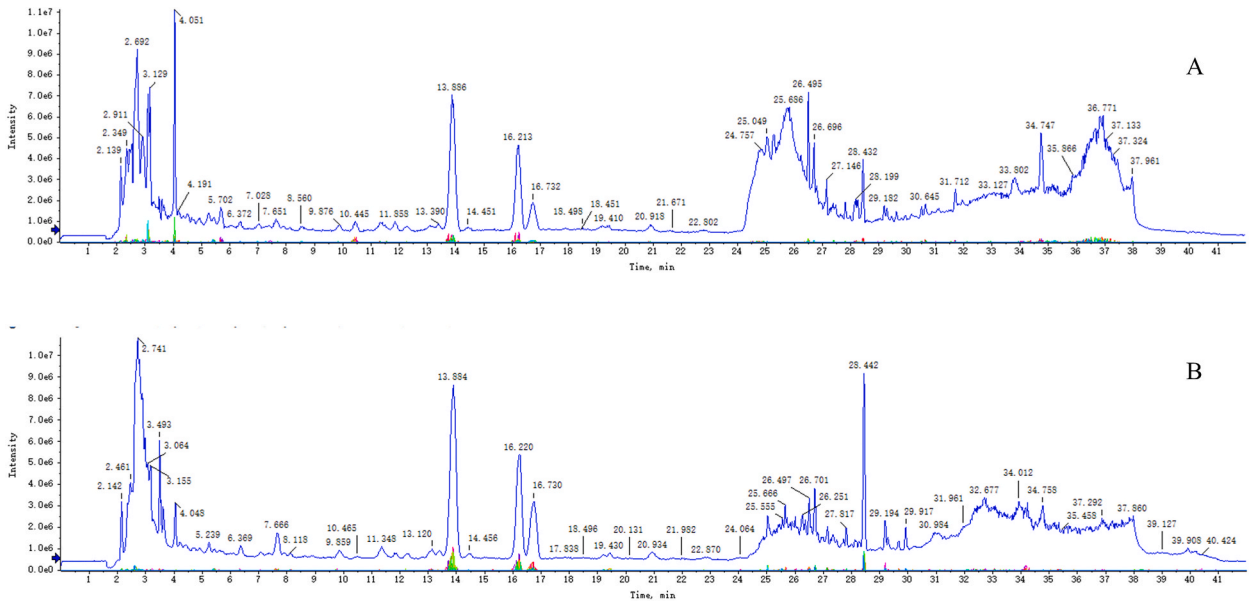

Fig. 1. TICs of GSDG in the positive (A) and negative (B) mode.

second pathway was associated with the formation of the base peak ion $[M+H-H_2O-HCOOH]^+$ at *m/z* 84.0482 along with $[M+H-H_2O-HCOOH-CO]^+$ at *m/z* 56.0562. For C5, some similar product ions were detected, including $[M+H-CO]^+$ (*m/z* 102.0623), $[M+H-HCOOH]^+$ (*m/z* 84.0484) and $[M+H-HCOOH-CO]^+$ (*m/z* 56.0568). By comparison with their reference standards, C5 and C6 were identified to be pyroglutamic acid and glutamic acid, respectively [12].

3.1.2. Organic acids

In GSDG, a total of 9 organic acids were identified in the negative ion mode. These components experienced cleavages by losing HCOOH, CO_2 (44 Da), CO or H_2O, consistent with the characteristic fragmentation of carboxylic groups which are the common structure of organic acids.

The molecular formula of C35 was determined to be $C_{11}H_{12}O_6$, due to its precursor ion at *m/z* 239.0557 $[M-H]^-$. Two initial fragment ions at *m/z* 221.0455 $[M-H-H_2O]^-$ and 195.0660 $[M-H-CO_2]^-$ resulted from the dehydration and decarbonation reactions of $[M-H]^-$, respectively. A common and fundamental intermediate ion $[M-H-H_2O-CO_2]^-$ (or $[M-H-CO_2-H_2O]^-$) was generated at *m/z* 177.0550 due to the further loss of a CO_2 or a H_2O moiety. After the individual elimination of a CO unit and a CO_2 unit, the intermediate was converted into $[M-H-H_2O-CO_2-CO]^-$ (*m/z* 149.0606) and $[M-H-H_2O-CO_2-CO_2]^-$ (*m/z* 133.0657), respectively. Then, a neutral loss of a $CH_2{=}C{=}CH_2$ unit happened to the latter ion, producing $[M-H-H_2O-CO_2-CO_2-C_3H_4]^-$ at *m/z* 93.0361. Besides, a CH≡COH group was speculated to fall out of the benzene ring, which took place on $[M-H-H_2O]^-$ and $[M-H-CO_2-H_2O-CO]^-$, resulting in two product ions at *m/z* 179.0342 and 107.0506. Taken together, C35 was identified as eucomic acid [18,19]. Its MS/MS spectrum and proposed cleavage pathways are shown in Fig. 2.

C52 exhibited its quasi-molecular ion $[M-H]^-$ at *m/z* 277.1439, consistent with chemical formula of $C_{18}H_{30}O_2$. The two peaks at *m/z* 233.1537 and 121.0296 represented the two ions produced by the losses of a CO_2 group and a $C_9H_{16}O_2$ group on the benzene ring, respectively. Their common product ion was observed at *m/z* 77.0415 $[M-H-C_9H_{16}O_2-CO_2]^-$ (or $[M-H-CO_2-C_9H_{16}O_2]^-$). Due to the ester bond cleavage and rearrangement of the precursor ion, the third product ion was observed at *m/z* 147.0084 $[M-H-C_8H_{18}O]^-$. In addition, the loss of an alkyl side chain followed by the dehydrogenation resulted in a fragment ion at *m/z* 107.0510. Based on the published literature data, C52 might be monoethylhexyl phthalic acid [20,21].

C10 showed a deprotonated ion at *m/z* 191.0568 (base peak), suggesting its chemical formula was $C_7H_{12}O_6$. Its characteristic fragment ions were detected at *m/z* 173.0469 $[M-H-H_2O]^-$, 155.0421 $[M-H-2H_2O]^-$, 137.0282 $[M-H-3H_2O]^-$, 127.0393 $[M-H-H_2O-HCOOH]^-$, 111.0463 $[M-H-2H_2O-CO_2]^-$, and 93.0354 $[M-H-3H_2O-CO_2]^-$. Obviously, dehydration, decarboxylation and decarbonation were its dominant fragmentation pathways. C28 produced a parent ion $[M-H]^-$ at *m/z* 193.0519 ($C_{10}H_{10}O_4$), which further yielded diagnostic ions at *m/z* 178.0263 $[M-H-CH_3]^-$, 149.0579 $[M-H-CO_2]^-$, 134.0372 $[M-H-CH_3-CO_2]^-$, and 106.0422 $[M-H-CH_3-CO_2-CO]^-$. C31 provided its quasi-molecular ion $[M-H]^-$ at *m/z* 137.0244, consistent with a molecular formula of $C_7H_6O_3$. Its base peak ion was observed at *m/z* 93.0355 $[M-H-CO_2]^-$, with a fragment ion at *m/z* 65.0401 $[M-H-CO_2-CO]^-$. Based on their MS/MS data, C10, C12, C27, C28 and C31 were identified to be quinic acid, shikimic acid, vanillic acid, ferulic acid and salicylic acid, respectively [22–27], all of which were further confirmed by comparing with their reference standards.

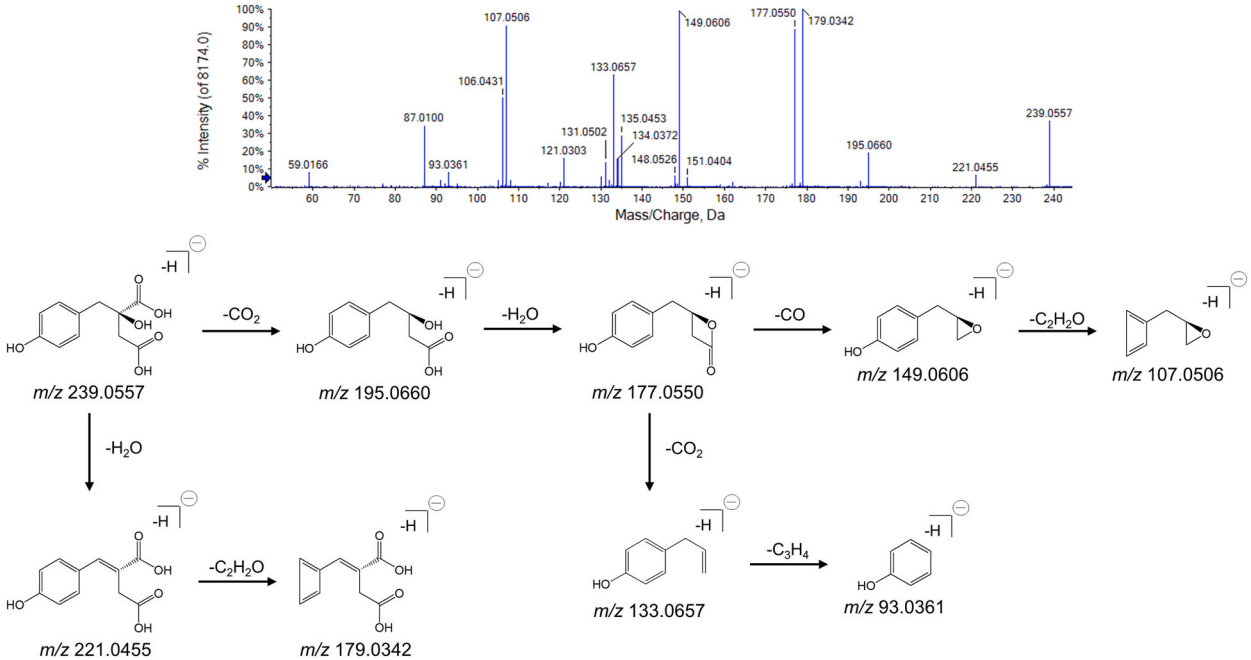

Fig. 2. MS/MS spectrum and proposed fragmentation pathway of eucomic acid.

3.1.3. Nucleosides and nucleobases

Similar to amino acids, both nucleosides and nucleobases are a group of nitrogenous substances common in botanicals. Three nucleobases and three nucleosides were identified in GSDG. The presence of the fragment ions, at *m/z* 268.1040 $[M+H]^+$, 136.0628 $[M+H-C_5H_8O_4]^+$, and 119.0370 $[M+H-C_5H_8O_4-NH_3]^+$ in the MS/MS spectrum of C15 indicated that it followed the characteristic cleavage pathways of the nucleosides, including the losses of a ribose unit ($C_5H_8O_4$, 132 Da) and an ammonia unit in the positive mode. C4 showed its characteristic fragment ions at *m/z* 136.0617 $[M+H]^+$, 119.0365 $[M+H-NH_3]^+$, and 92.0275 $[M+H-NH_3-HCN]^+$. C20 showed its characteristic fragment ions at *m/z* 152.0566 $[M+H]^+$, 135.0325 $[M+H-NH_3]^+$, and 107.0461 $[M+H-NH_3-CO]^+$. C22 showed its characteristic fragment ions at *m/z* 153.0431 $[M+H]^+$ and 136.0158 $[M+H-NH_3]^+$. The cleavage behaviors of the three components were consistent with those of nucleobases, involving the loss of an ammonia unit, a hydrocyanic acid (27 Da) or a carbonyl group. With these MS/MS information and the published data, C4, C15, C20, C22 were identified to be adenine, adenosine, guanine, xanthine, respectively [28].

C29 showed a protonated ion $[M+H]^+$ at *m/z* 352.1718, which produced a base peak ion at *m/z* 220.1170 $[M+H-C_5H_8O_4]^+$ by losing a ribose. This aglycone ion further underwent fragmentation via two cleavage pathways. The first involved dehydration and deamination, producing two fragment ions $[M+H-C_5H_8O_4-H_2O]^+$ and $[M+H-C_5H_8O_4-H_2O-NH_3]^+$ at *m/z* 202.1084 and 185.0847, respectively. The second was associated with the loss of a side chain on amidogen followed by the further deamination, contributing to $[M+H-C_5H_8O_4-C_5H_8O]^+$ at *m/z* 136.0649 and $[M+H-C_5H_8O_4-C_5H_8O-NH_3]^+$ at *m/z* 119.0425. Based on the above information, C29 was tentatively identified to be ribosylzeatin [29], a common plant growth regulator. Fig. 3 exhibits its MS/MS spectrum and proposed cleavage pathways.

3.1.4. Flavonoids

Flavonoids are the known fundamental substances in botanicals. The cleavage of the glycosidic bond which is characteristic to flavonoid glycosides and the losses of 146 Da, 162 Da, and 308 Da which are usually attributed to the rhamnose, glucose, and rutinose moieties, respectively [23,30,31], are important for structure identification of flavonoids. In GSDG, 6 flavonoids were identified as folows.

C38 showed its $[M-H]^-$ ion at *m/z* 609.0911, suggesting that its chemical formula was $C_{27}H_{30}O_{16}$. An aglycone ion at *m/z* 301.0086 indicated the loss of a rutinose. As another fragment ion at *m/z* 300.0003 had a higher relative intensity than the ion at *m/z* 301.0086, C38 was speculated to be 3-*O*-rutinoside. RDA reaction and rearrangement were found to be the predominant cleavage pattern for this aglycone ion. Due to the two different RDA cleavages, two different fragment ions were yielded at *m/z* 150.9897 and 107.0038, respectively. The third pattern caused two product ions at *m/z* 178.9813 and 121.0172. These results revealed that the aglycone might be quercetin. In addition, three other fragment ions at *m/z* 271.0004, 255.0078 and 243.0183, corresponding to

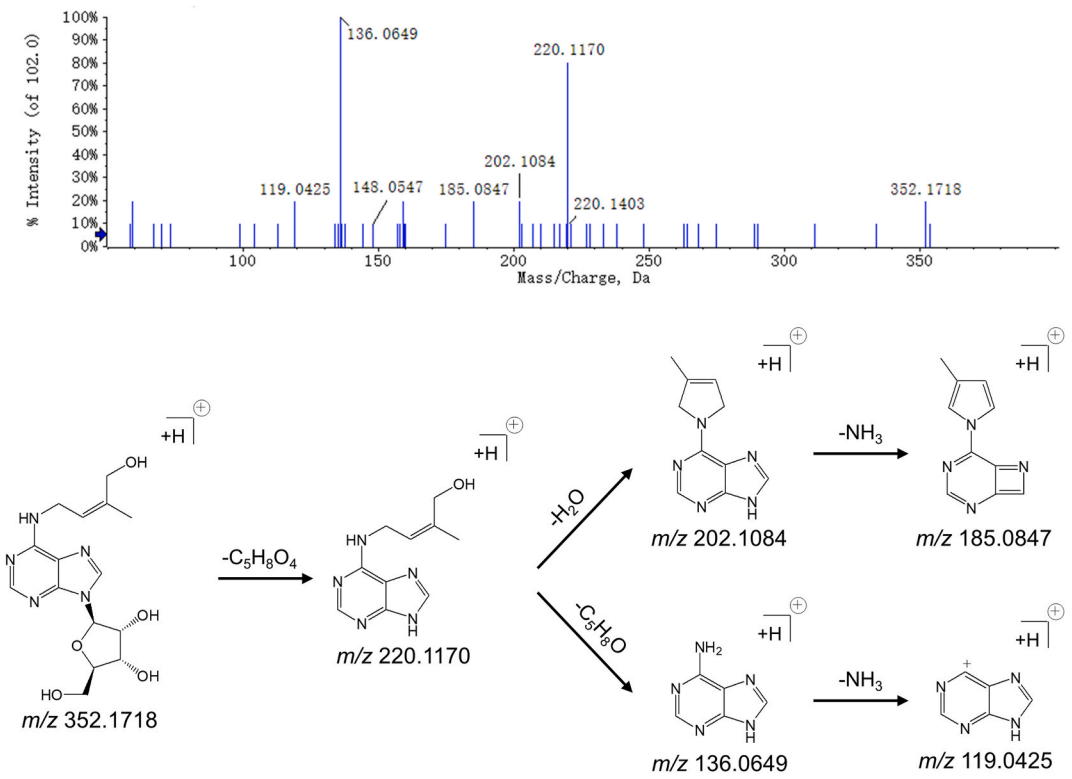

Fig. 3. MS/MS spectrum and proposed fragmentation pathway of ribosylzeatin.

$[M-H-Rut-H-CO-H]^-$, $[M-H-Rut-H-CO-OH]^-$ and $[M-H-Rut-H-CO-H-CO]^-$, respectively, confirmed the above speculation. By comparison with its reference standard, C38 was identified to be rutin [32,33]. Its MS/MS spectrum and proposed cleavage pathways are presented in Supplementary Fig. 2. Both C39 and C40 were also 3-*O*-rutinosides due to the presence of ion pairs of the deprotonated ion and desugarization ion at *m/z* 593.0964 and 285.0151 and at *m/z* 623.1117 and 315.0248, respectively. Based on these accurate molecular weights and fragmentation behaviors, and in conjunction with the published data, C39 and C40 were identified to be nicotiflorin and narcissin, respectively [34,35].

C50 and C53 shared a common chemical formula $C_{15}H_{10}O_5$ because their deprotonated ions $[M-H]^-$ were detected at *m/z* 269.0425 and 269.0446, respectively. The consecutive elimination of a CO group and an oxygen atom led to the product ions at *m/z* 241.0506 and 225.0520 for C50 and at *m/z* 241.0519 and 225.0551 for C53, respectively. In addition, the formation of a group of diagnostic ions at *m/z* 151.0718 and 117.0328 for C50 and at *m/z* 151.0555, 117.0346, and 107.0195 for C53 revealed RDA fragmentation pathways. Based on the published data, C50 and C53 were identified to be genistein and apigenin, respectively [36–38], both of which were confirmed by comparison with their reference standards.

3.1.5. Vitamins

In GSDG, 5 vitamins were detected, including vitamin B2, vitamin B3, vitamin B5, vitamin B6, and vitamin H.

C26 showed its quasi-molecular ion at *m/z* 220.1193 in the positive mode, consistent with a chemical formula of $C_9H_{17}NO_5$. On account of several hydroxyl groups, several dehydration product ions were observed at *m/z* 202.1084 $[M+H-H_2O]^+$, 184.0968 $[M+H-2H_2O]^+$, and 166.0945 $[M+H-3H_2O]^+$ due to the losses of one, two, and three H_2O units, respectively. The third product ion further lost a C_6H_7NO unit and a C_5H_8 unit to produce the fragment ions at *m/z* 57.0772 $[M+H-3H_2O-C_6H_7NO]^+$ and 98.0264 $[M+H-3H_2O-C_5H_8]^+$, respectively. Two fragment ions at *m/z* 156.1005 ($[M+H-2H_2O-CO]^+$) and 142.0851 ($[M+H-2H_2O-CO-CH_2]^+$) arose from the sequential losses of a CO unit and a CH_2 unit from $[M+H-2H_2O]^+$. For the latter, two downstream ions were observed at *m/z* 124.0780 and 70.0343, owing to the losses of a H_2O moiety and a C_4H_8O group (72 Da), respectively. In addition, the production of two product ions at *m/z* 90.0593 and 72.0505 were due to the breaking of amido bond accompanied with the loss of a $C_6H_{10}O_3$ (130 Da) group from $[M+H]^+$ and $[M+H-H_2O]^+$, respectively. Based on these accurate molecular weights and proposed fragmentation pathways (Fig. 4), C26 was temporarily assigned as pantothenic acid (vitamin B5) [39,40]. C13 showed its protonated ion at *m/z* 124.0397, consistent with a chemical formula of $C_6H_5NO_2$. Three cleavage pathways, i.e., dehydration, decarbonation and decarboxylation, resulted in three different product ions at *m/z* 106.0307 ($[M+H-H_2O]^+$), 80.0531 ($[M+H-CO_2]^+$) and 78.0383 ($[M+H-HCOOH]^+$), respectively. All three ions further underwent decyanation to form their respective homologous products at *m/z* 79.0462 ($[M+H-H_2O-HCN]^+$), 53.0459 ($[M+H-CO_2-HCN]^+$) and 51.0313 ($[M+H-HCOOH-HCN]^+$). According to its MS/MS spectrum and proposed fragmentation pathway as shown in Supplementary Fig. 3, C13 might be nicotinic acid (vitamin B3) [37,41]. Additionally, C14, C23 and C36 were speculated to be pyridoxal (a form of vitamin B6), biotin (vitamin H) and riboflavin (vitamin B2) because their quasi-molecular ions $[M+H]^+$ were detected at *m/z* 168.0655 ($C_8H_9NO_3$), 245.0954 ($C_{10}H_{16}N_2O_3S$) and 377.1483 ($C_{17}H_{20}N_4O_6$), respectively [42–44].

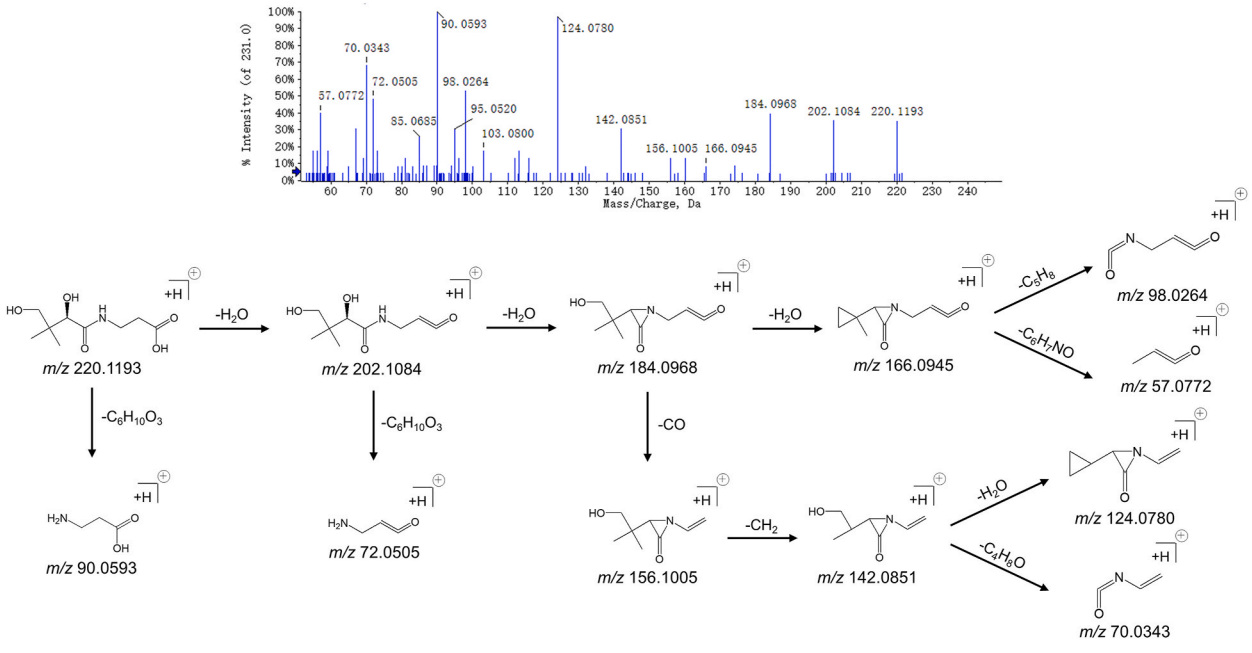

Fig. 4. MS/MS spectrum and proposed fragmentation pathway of vitamin B5.

3.1.6. Terpenoid lactones

As is known, terpenoid lactones are the major bioactive components of the plant *Ginkgo biloba*. These components are characterized with three lactonic rings and many hydroxyl groups in their chemical structures. Therefore, the opening of the lactonic rings and sequential elimination of CO_2, CO, and H_2O represent the typical fragmentation pathways in the MS/MS spectra. For example, C41 showed its deprotonated ion $[M-H]^-$ at *m/z* 439.1237, consistent with a chemical formula of $C_{20}H_{24}O_{11}$. In the high-weight region of the MS/MS spectrum, the major fragment ions, which followed the breaking patterns above mentioned, were observed at *m/z* 411.1287, 383.1336, 365.1220, 321.1342, 303.1220, 277.1433, 259.1346 and 241.1244, corresponding to $[M-H-CO]^-$, $[M-H-2CO]^-$ (base peak), $[M-H-2CO-H_2O]^-$, $[M-H-2CO-H_2O-CO_2]^-$, $[M-H-2CO-H_2O-CO_2-H_2O]^-$, $[M-H-2CO-H_2O-2CO_2]^-$, $[M-H-2CO-H_2O-2CO_2-H_2O]^-$ and $[M-H-2CO-H_2O-2CO_2-2H_2O]^-$, respectively. In addition, there were several cleavage-induced residue ions at *m/z* 141.0191 ($[C_6H_5O_4^-]^-$), 125.0246 ($[C_6H_5O_3^-]^-$), 113.0244 ($[C_5H_5O_3^-]^-$), 97.0301 ($[C_5H_5O_2^-]^-$) and 72.9948 ($[C_2HO_3^-]^-$). Among them, the last one was the ring-opening product arisen from a five-membered lactonic ring and was also found in the spectrum of C42 (*m/z* 72.9959), C44 (*m/z* 72.9952), C45 (*m/z* 72.9950), and C46 (*m/z* 72.9941). Thus, the fragment ion at *m/z* 72.99 was considered as the diagnostic ion for this category of phytochemicals. As shown in Table 2, C44 (or C45) demonstrated a mass difference of 16 Da (O) from C41 between the precursor ion and many product ions. Hence, C41 was deduced to be ginkgolide C [45–47]. Its MS/MS spectrum and proposed fragmentation pathways are demonstrated in Fig. 5. C42, C44, C45, and C46 showed their protonated ions at *m/z* 325.0929, 423.1344, 423.1278 and 407.1347, respectively. According to their accurate molecular weights, the chemical formulas of C42, C44, C45 and C46 might be $C_{15}H_{18}O_8$, $C_{20}H_{24}O_{10}$, $C_{20}H_{24}O_{10}$ and $C_{20}H_{24}O_9$, respectively. Because of the similar fragmentation pathways and residue ions as above mentioned, C42, C44, C45, and C46 were identified as bilobalide, ginkgolide J, ginkgolide B, and ginkgolide A, respectively [48–50]. These terpenoid lactones were further confirmed by comparison with their reference standards.

3.1.7. Carbohydrates

In the negative mode, C9 showed its quasi-molecular ion at *m/z* 179.0567, consistent with a molecular formula of $C_6H_{12}O_6$, a typical saccharide with the unsaturation degree of 1. Due to the presence of some hydroxyl groups, the loss of a H_2O moiety was often observed. The initial dehydration product ion $[M-H-H_2O]^-$ (*m/z* 161.0465) seemed very important because it underwent further fragmentation through four possible downstream cleavage pathways. As for the first two, the further loss of a CH_3OH unit led to a fragment ion at *m/z* 129.0197 $[M-H-H_2O-CH_3OH]^-$ and the further loss of a H_2O moiety produced a fragment ion at *m/z* 143.0381 $[M-H-2H_2O]^-$. For the third pathway, an intermediate deformylation product ion $[M-H-H_2O-HCHO]^-$ was detected at *m/z* 131.0355 and two end product ions were observed at *m/z* 85.0306 and 113.0928, corresponding to $[M-H-H_2O-HCHO-H_2O-CO]^-$ and $[M-H-H_2O-HCHO-H_2O]^-$, respectively. The fourth pathway mainly involved the sequential losses of a C_2H_2O unit and a H_2O molecule, generating an intermediate product ion $[M-H-H_2O-C_2H_2O-H_2O]^-$ with a four-membered ring at *m/z* 101.0232. Two end product ions at *m/z* 83.0140 and 59.0152 were attributed to the individual loss of a H_2O moiety and a C_2H_2O unit, respectively. Therefore, C9 was speculated to be a hexose [51,52]. Based on the limited information about its configuration obtained from the MS/MS spectrum, C9 was temporarily identified to be glucose, fructose or mannose. Supplementary Fig. 4 exhibits the MS/MS spectrum and proposed cleavage pathways of C9 assumed to be glucose. According to their accurate molecular masses of 503.1617 and 341.1073 in the negative mode, C7 and C8 were regarded as $C_{18}H_{32}O_{16}$ and $C_{12}H_{22}O_{11}$, respectively. In their spectra, the fragment ions of a hexose, which were consistent with the cleavage pathways of a monosaccharide like C9, were also shown at *m/z* 179.0579, 161.0428, 143.0371, 101.0232, 89.0287, 73.0325, and 59.0159 for C7, and at *m/z* 179.0546, 161.0435, 143.0353, 101.0241, 89.0247, 85.0320, 71.0146, and 59.0159 for C8. In addition, a mass gap of 162 Da was common among *m/z* 503.1617, 341.1124 and 179.0579, among *m/z* 425.1368, 263.0762 and 101.0232, and among *m/z* 383.1201, 221.0650 and 59.0159 for C7, as well as between *m/z* 341.1073 and 179.0546, and between *m/z* 263.0828 and 101.0241 for C8. Accordingly, C7 and C8 were tentatively assigned as raffinose (a trisaccharide) and sucrose (a disaccharide) [53–55].

3.1.8. Other compounds

In addition to the categories listed above, another 9 compounds were identified in GSDG, as detailed below. As a special component, C33 showed its protonated ion $[M-H]^-$ at *m/z* 451.1347, consistent with a molecular formula of $C_{20}H_{24}N_2O_{10}$. The dehydration between two carboxyl groups produced a product ion containing succinic anhydride at *m/z* 433.1241 $[M-H-H_2O]^-$. Additional two initial fragment ions, corresponding to $[M-H-CO_2]^-$ and $[M-H-HOOCCH=CHCOOH]^-$, respectively, were observed at *m/z* 407.1451 and 335.1234 in the MS/MS spectrum. The further losses of a glucose group (162 Da) and a CONH group (43 Da) were also observed in the MS/MS spectrum. Depending on the loss sequence, two intermediate ions were produced at *m/z* 173.0711 (base peak) and 292.1181, respectively, and a common end product ion was obtained at *m/z* 130.0660 $[M-H-HOOCCH=CHCOOH-C_6H_{10}O_5-CONH]^-$., A fragment ion at *m/z* 156.0452 $[M-H-HOOCCH=CHCOOH-C_6H_{10}O_5-NH_3]^-$ was formed due to the loss of a NH_3 moiety from the base peak. Furthermore, two product ions at *m/z* 128.0504 and 101.0250 arose from the sequential elimination of a CO unit and a HCN moiety. On the other hand, the quasi-molecular ion of C34 was detected at *m/z* 465.1506 in the negative mode, consistent with a chemical formula of $C_{21}H_{26}N_2O_{10}$. Two product ions, which resulted from two different fragmentation pathways, were observed at *m/z* 447.1416 $[M-H-H_2O]^-$ and 421.1628 $[M-H-CO_2]^-$, respectively. These three ions were found to have a common distance of 14 Da (CH_2) to those of C33, indicating that the two components might be the neighboring homologues. The third ion was further converted into a product ion at *m/z* 259.1095 after a further deglycosylation. Additionally, several fragment ions detected at *m/z* 292.1197 $[M-H-CO_2-C_5H_7NO_3]^-$, 173.0736 $[M-H-CO_2-C_6H_{10}O_5-CH_3CH=CHCOOH]^-$, 156.0449 $[M-H-CO_2-C_6H_{10}O_5-CH_3CH=CHCOOH-NH_3]^-$, 128.0360 $[M-H-CO_2-C_6H_{10}O_5-CH_3CH=CHCOOH-NH_3-CO]^-$, and 101.0254 $[M-H-CO_2-C_6H_{10}O_5-CH_3CH=CHCOOH-NH_3-CO-HCN]^-$ were found to be similar to C33. C33 and C34 were temporarily deduced to be *N*-(*N*-glucopyranosyl)-indoleacetylaspartate and *N*-(*N*-glucopyranosyl)-indoleacetylglutamate, respectively [56]. The MS/MS spectrum and proposed fragmentation pathway of C33 are

Table 2
Chemical constituents identified in GSDG by HPLC-QTOF-MS.

No.	RT (min)	Molecular formula	MS/MS fragments	Mode	Error (ppm)	Identification
1	2.31	$C_6H_{14}N_4O_2$	175.1189, 158.0925, 130.0086, 116.0723, 70.0703, 60.0620	+	−3.0	Arginine
2	2.34	$C_5H_9NO_2$	116.0826, 70.0702	+	0.8	Proline
3	2.37	$C_6H_9N_3O_2$	156.0767, 155.9004, 114.9519, 72.9433	+	−2.0	Histidine[a]
4	2.68	$C_5H_5N_5$	136.0617, 119.0365, 94.0426, 92.0275	+	−1.0	Adenine
5	2.71	$C_5H_7NO_3$	130.0514, 102.0623, 85.8761, 84.0484, 70.0705, 56.0568	+	0.6	Pyroglutamic acid[a]
6	2.73	$C_5H_9NO_4$	148.0613, 130.0517, 102.0580, 85.0318, 84.0482, 56.0562	+	−1.0	Glutamic acid[a]
7	2.78	$C_{18}H_{32}O_{16}$	503.1617, 425.1368, 383.1201, 341.1124, 281.0843, 263.0762, 221.0650, 179.0579, 161.0428, 143.0371, 101.0232, 89.0287, 73.0325, 59.0159	–	−0.8	Raffinose
8	2.86	$C_{12}H_{22}O_{11}$	341.1073, 263.0828, 179.0546, 161.0435, 143.0353, 119.0353, 113.0243, 101.0241, 89.0247, 85.0320, 71.0146, 59.0159	–	−0.8	Sucrose
9	2.93	$C_6H_{12}O_6$	179.0567, 161.0465, 143.0381, 131.0355, 129.0197, 113.0928, 101.0232, 89.0277, 85.0306, 83.0140, 71.0130, 59.0152, 57.0379	–	4.0	Glucose or Mannose or Fructose
10	2.96	$C_7H_{12}O_6$	191.0568, 173.0469, 155.0421, 137.0282, 127.0393, 111.0463, 93.0354, 87.0092, 85.0310, 59.0163	–	5.9	Quinic acid[a]
11	2.99	$C_5H_{11}NO_2$	118.0862, 72.0857, 58.0709, 57.0631, 56.0557, 55.0608, 54.8879	+	−0.3	Valine
12	3.13	$C_7H_{10}O_5$	173.0455, 154.9999, 111.0092, 99.0093, 85.0313, 83.0123, 72.9930	–	5.1	Shikimic acid[a]
13	3.61	$C_6H_5NO_2$	124.0397, 106.0307, 80.0531, 79.0462, 78.0383, 53.0459, 51.0313	+	−0.6	Nicotinic acid (Vitamin B3)
14	3.71	$C_8H_9NO_3$	168.0655, 122.0658, 94.9876	+	−0.7	Pyridoxal (Vitamin B6)
15	3.79	$C_{10}H_{13}N_5O_4$	268.1040, 136.0628, 119.0370	+	0.4	Adenosine
16	3.92	$C_5H_{11}NO_2S$	150.0583, 133.0331, 102.0552, 90.9187, 84.0493, 74.0259, 61.0275, 56.0543	+	−7.1	Methionine
17	4.08	$C_9H_{13}NO_3$	184.1055, 152.0713, 134.0617, 124.0774, 106.0661, 94.0690, 80.0536, 77.0431, 65.0458	+	−1.5	4′-*O*-methylpyridoxine (Ginkgotoxin)[a]
18	4.13	$C_6H_{13}NO_2$	132.1017, 90.9121, 86.1002, 85.8403, 69.0738, 57.0719, 55.0211, 53.0063	+	−0.6	Leucine
19	4.27	$C_6H_{13}NO_2$	132.1016, 86.1002, 72.9421, 69.0739, 55.0676	+	−0.6	Isoleucine
20	4.43	$C_5H_5N_5O$	152.0566, 135.0325, 123.0716, 110.0351, 107.0461, 93.0130, 67.0391, 65.0644	+	1.4	Guanine
21	4.97	$C_9H_{11}NO_3$	182.0759, 136.0798, 122.0623, 119.0534, 93.0638, 91.0572, 77.0407, 67.0654	+	−1.2	Tyrosine
22	5.02	$C_5H_4N_4O_2$	153.0431, 136.0158, 110.0364, 93.0082, 82.0487, 81.0113, 53.0199	+	−6.1	Xanthine
23	5.05	$C_{10}H_{16}N_2O_3S$	245.0954, 124.6801, 98.0588, 80.0503, 68.0536	+	7.3	Biotin (Vitamin H)
24	5.31	$C_6H_{13}NO_5$	180.0866, 162.0771, 137.0823, 135.0303, 122.0618, 107.0379, 71.0657	+	4.0	Galactosamine
25	5.66	$C_9H_{11}NO_2$	166.0926, 120.0830, 107.0535, 103.0571, 93.0731, 91.0579, 79.0591, 77.0434, 51.0303	+	−1.7	Phenylalanine
26	6.09	$C_9H_{17}NO_5$	220.1193, 202.1084, 184.0968, 166.0945, 156.1005, 142.0851, 124.0780, 98.0264, 90.0593, 72.0505, 70.0343, 57.0772	+	0.1	Pantothenic acid (Vitamin B5)[a]
27	6.33	$C_8H_8O_4$	167.0319, 166.8347, 152.0107, 108.0201	–	7.8	Vanillic acid[a]
28	7.67	$C_{10}H_{10}O_4$	193.0519, 178.0263, 149.0579, 134.0372, 106.0422	–	5.5	Ferulic acid[a]
29	11.27	$C_{15}H_{21}N_5O_5$	352.1718, 220.1170, 202.1084, 185.0847, 159.0744, 148.0547, 136.0649, 119.0425	+	−0.5	Ribosylzeatin
30	13.12	$C_{16}H_{20}O_9$	355.1034, 193.0502, 149.0603	–	−0.4	*trans*-Ferulic acid-4-*O*-*β*-D-glucoside
31	13.67	$C_7H_6O_3$	137.0244, 93.0355, 65.0401	–	5.9	Salicylic acid[a]
32	13.88	$C_4H_7NO_4$	134.0445, 74.0323, 70.0421, 57.9431, 55.9573	+	−0.9	Aspartic acid[a]
33	13.90	$C_{20}H_{24}N_2O_{10}$	451.1347, 433.1241, 407.1451, 335.1234, 292.1181, 173.0711, 156.0452, 132.0297,	–	−0.4	*N*-(*N*-glucopyranosyl)-indoleacetylaspartate[a]

(*continued on next page*)

Table 2 (*continued*)

No.	RT (min)	Molecular formula	MS/MS fragments	Mode	Error (ppm)	Identification
			130.0660, 128.0504, 101.0250, 88.0411, 71.0155			
34	16.07	$C_{21}H_{26}N_2O_{10}$	465.1506, 447.1416, 421.1628, 336.1095, 292.1197, 259.1095, 173.0736, 156.0449, 146.0464, 128.0360, 101.0254	–	−2.8	*N*-(*N*-glucopyranosyl)-indoleacetylglutamate[a]
35	16.73	$C_{11}H_{12}O_6$	239.0557, 221.0455, 195.0660, 179.0342, 177.0550, 149.0606, 148.0526, 135.0453, 133.0657, 121.0303, 107.0506, 106.0431, 93.0361, 87.0100, 59.0166	–	2.3	Eucomic acid[a]
36	20.44	$C_{17}H_{20}N_4O_6$	377.1483, 359.1168, 243.0882, 198.0661, 172.0895, 145.0696, 118.0688, 77.0374, 57.0363	+	0.5	Riboflavin (Vitamin B2)
37	21.26	C_8H_{10}	107.0855, 91.0593, 77.0401, 65.0474	+	1.4	Xylene
38	25.90	$C_{27}H_{30}O_{16}$	609.0911, 301.0086, 300.0003, 271.0004, 255.0078, 243.0183, 178.9813, 150.9897, 121.0172, 107.0038	–	−3.6	Rutin[a]
39	26.43	$C_{27}H_{30}O_{15}$	593.0964, 285.0151, 284.0075, 255.0071, 229.0299, 187.0398	–	−4.6	Nicotiflorin
40	26.50	$C_{28}H_{32}O_{16}$	623.1117, 315.0248, 314.0170, 300.0026, 285.0165, 271.0022, 255.0085, 243.0096	–	−2.7	Narcissin
41	26.70	$C_{20}H_{24}O_{11}$	439.1237, 411.1287, 383.1336, 365.1220, 321.1342, 303.1220, 277.1433, 259.1346, 241.1244, 141.0191, 125.0246, 113.0244, 97.0301, 72.9948	–	−2.1	Ginkgolide C[a]
42	27.08	$C_{15}H_{18}O_8$	325.0929, 307.0845, 219.1016, 193.1229, 191.1073, 175.1127, 165.0555, 136.0523, 135.0145, 118.0418, 107.0501, 99.0823, 72.9959	–	0.9	Bilobalide[a]
43	27.82	$C_{14}H_{20}O_6$	283.1187, 265.1099, 221.1147, 195.0462, 180.0253, 179.1038, 145.0253, 121.0297, 72.9954	–	0.1	2- Phenylethyl-*β*-D-glucopyranoside
44	28.03	$C_{20}H_{24}O_{10}$	423.1344, 395.1167, 367.1394, 349.1308, 331.1178, 287.1280, 261.1510, 243.1384, 215.1450, 186.0864, 149.0976, 99.0853, 83.0558, 72.9952	–	−2.6	Ginkgolide J[a]
45	28.41	$C_{20}H_{24}O_{10}$	423.1278, 395.1331, 367.1381, 349.1279, 305.1385, 287.1275, 261.1492, 243.1390, 141.0186, 125.0247, 113.0247, 72.9950	–	−2.6	Ginkgolide B[a]
46	29.66	$C_{20}H_{24}O_9$	407.1347, 379.1385, 351.1439, 333.1359, 307.1559, 289.1432, 263.1644, 245.1542, 72.9941	–	−2.8	Ginkgolide A[a]
47	30.28	$C_{13}H_{20}O$	193.1586, 107.0907, 67.0571, 55.0621	+	0.1	Ionone
48	30.47	$C_9H_{13}N_3O_4$	226.0950, 93.0237	–	−0.2	2′-Deoxycytidine
49	30.63	$C_{30}H_{26}O_{13}$	593.1300, 165.0209, 121.0330	–	−4.4	Procyanidin
50	30.80	$C_{15}H_{10}O_5$	269.0425, 241.0506, 225.0520, 197.0574, 182.0352, 151.0718, 117.0328	–	−0.4	Genistein[a]
51	31.13	$C_{18}H_{28}O_2$	277.2162, 235.1667, 145.0991, 93.0696, 79.0613, 67.0541	+	0.5	5, 12-Octadecadiynoic acid
52	31.96	$C_{18}H_{30}O_2$	277.1439, 233.1537, 147.0084, 134.0373, 127.1128, 121.0296, 119.0135, 107.0510, 77.0415, 75.0256	–	1.0	Monoethylhexyl phthalic acid
53	32.44	$C_{15}H_{10}O_5$	269.0446, 241.0519, 225.0551, 197.0595, 181.1653, 151.0555, 117.0346, 107.0195	–	−0.4	Apigenin[a]
54	34.56	$C_{13}H_{22}O$	195.1743, 95.0887, 81.0726, 69.0826, 67.0576, 55.0576	+	−3.2	Nerylacetone
55	37.11	$C_{21}H_{24}O_5$	356.1623, 311.1666, 309.3121, 293.1486	–	0.9	Myricanone
56	39.67	$C_{15}H_{24}$	205.1950, 149.0224, 121.0366, 107.0840, 69.0826, 57.0760	+	−1.3	Ylangene

[a] compared with its reference standard.

demonstrated in Fig. 6.

As shown in Fig. 7, C17 exhibited its quasi-molecular ion at *m/z* 184.1055 $[M+H]^+$ and an initial ion at *m/z* 152.0713 $[M+H-CH_3OH]^+$ in the positive mode. Two different fragmentation pathways were found to be responsible for two different intermediate ions (*m/z* 124.0774 $[M+H-CH_3OH-CO]^+$ and 134.0617 $[M+H-CH_3OH-H_2O]^+$) and a common product ion $[M+H-CH_3OH-H_2O-CO]^+$ at *m/z* 106.0661. This product ion further produced $[M+H-CH_3OH-H_2O-CO-C_2H_2]^+$ at *m/z* 80.0536 by losing a C_2H_2 unit and $[M+H-CH_3OH-H_2O-CO-HCN-H_2]^+$ at *m/z* 77.0431 by decyanation and dehydrogenation. Accordingly, C17 was identified to be 4′-*O*-methylpyridoxine (ginkgotoxin) [57,58], which was confirmed by comparison with its reference standard and the published data.

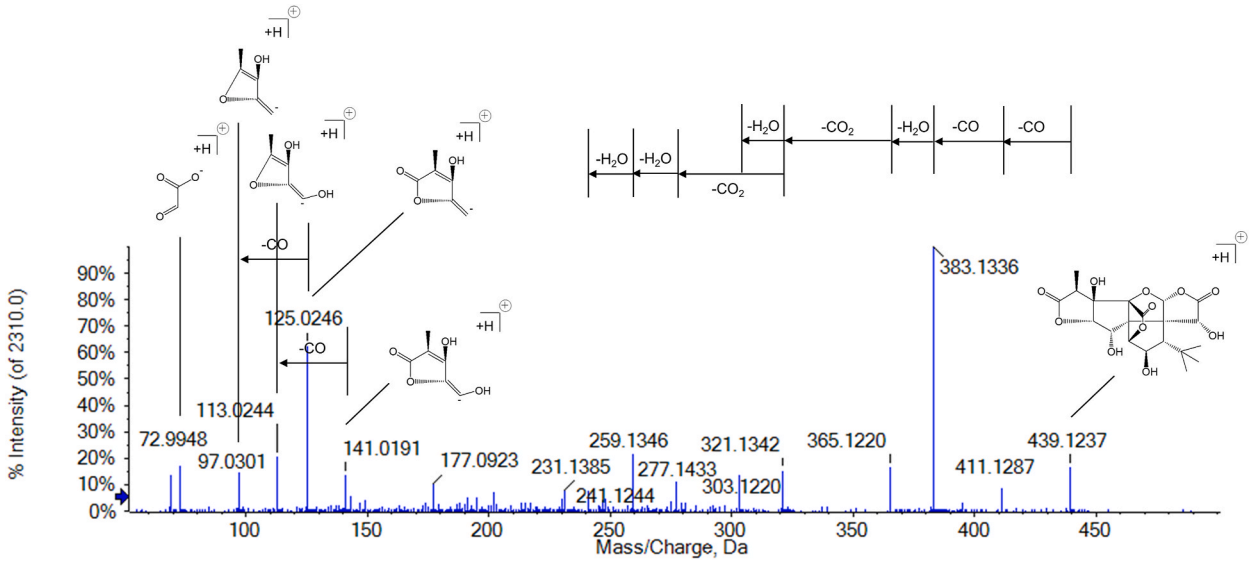

Fig. 5. MS/MS spectrum and proposed fragmentation pathway of ginkgolide C.

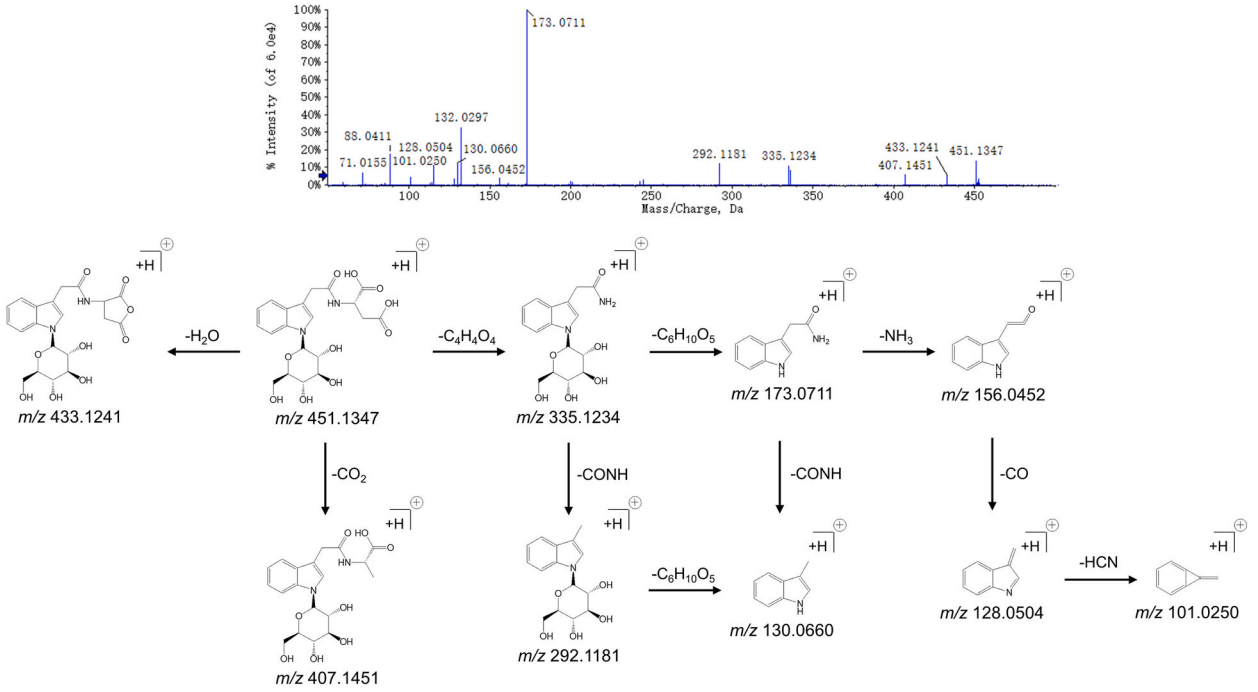

Fig. 6. MS/MS spectrum and proposed fragmentation pathway of *N*-(*N*-glucopyranosyl)-indolylacetylaspartate

3.2. Quantitative analysis

3.2.1. Selection and justification of the analytes

Ten representative biological active components were selected for quantification by HPLC-QTRAP-MS as the quality indicators of GSDG. The terpenoid lactones have shown the considerable effects on the pulmonary diseases. Ginkgolide C was documented to alleviate acute lung injury caused by paraquat poisoning via regulating the Nrf2 and NF-κB signaling pathways and to mitigate tumourigenesis in non-small cell lung cancer through abrogation of STAT3 activation cascade [59,60]. Ginkgolide B could protect human A549 cells from lipopolysaccharide-induced inflammatory responses by reducing TRIM37-mediated NF-κB activation [61]. Ginkgolide A treatment was documented to be effective in a murine model of neutrophil-predominant asthma through inhibiting

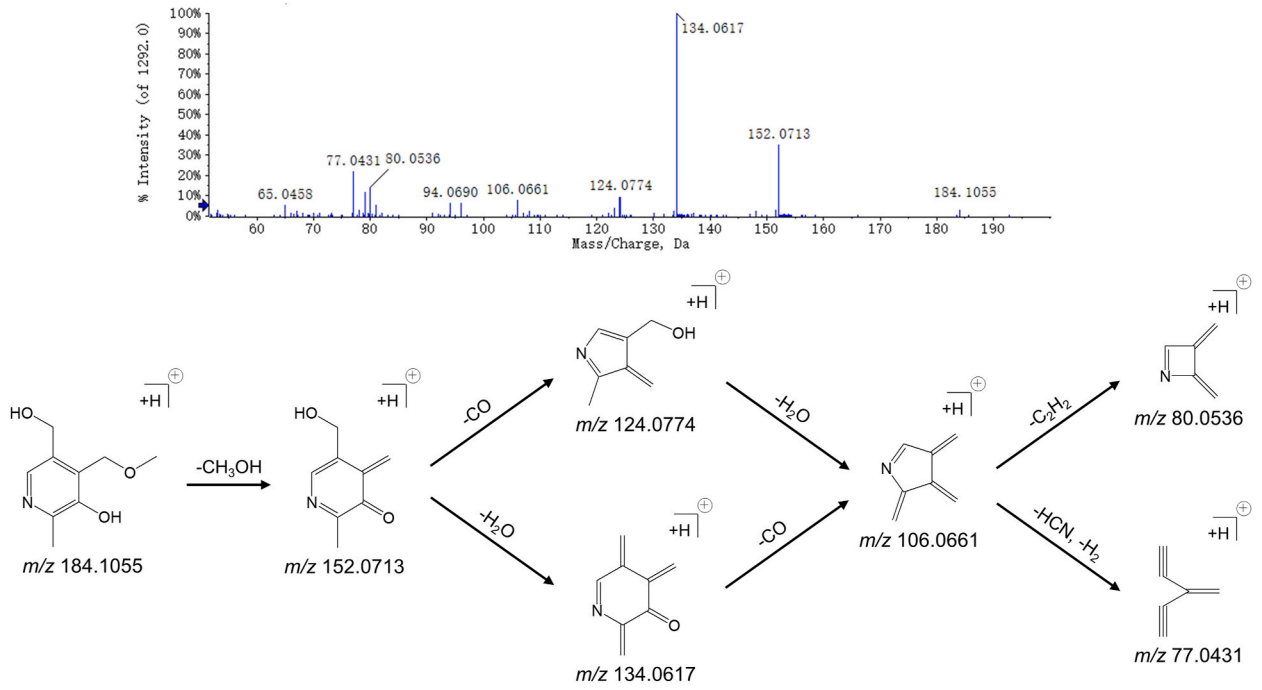

Fig. 7. MS/MS spectrum and proposed fragmentation pathway of ginkgotoxin.

response in the immune Th17 cells [62]. Among amino acids, histidine could improve lung function and ameliorate lung inflammation by inhibiting the activation of the NLRP3 inflammasome of the mice with chronic obstructive pulmonary disease [63]. Glutamic acid was reported to inhibit free radical processes, protect and mitigate CCl_4-induced oxidative stress in the lung tissues of male rats [64]. Both *N*-(*N*-glucopyranosyl)-indoleacetylaspartate and *N*-(*N*-glucopyranosyl)-indoleacetylglutamate were also reported to be antitussive compounds [56,65], while eucomic acid had the potential to increase the activity or expression of cytochrome *c* oxidase in human immortalized keratinocyte cell line (HaCaT) [66]. Furthermore, *N*-(*N*-glucopyranosyl)-indoleacetylaspartate, *N*-(*N*-glucopyranosyl)-indoleacetylglutamate and eucomic acid were selected because they contributed three dominating common peaks observed in the HPLC fingerprint chromatogram of GSDG (Supplementary Fig. 5).

3.2.2. Method validation

The regression equation and linear range derived for each analyte are summarized in Table 3, along with the limit of quantitation (LOQ) and limit of detection (LOD). The signal-noise ratios at LOQ and LOD levels were 10 and 3, respectively. With the coefficient of correlation (R^2) $\geq$ 0.99 for all analytes, the method is linear for the determination of each analyte in the given range.

The results obtained from the precision, stability, repeatability, and recovery tests are present in Table 4. The RSD values for precision and stability were within 1.35 %–4.52 % and 1.49 %–5.54 %, respectively. The repeatability RSD values ranged from 1.90 % to 4.46 %. The average method recoveries ranged from 88.84 % to 104.74 % (RSDs ≤5.60 %). Taken together, this method is shown to be accurate, sensitive, reproducible and suitable for the determination of the 10 selected markers in GSDG.

3.2.3. Method application

Ten batches of GSDG were quantitatively tested for 10 indicator components by the validated HPLC-QTRAP-MS. The MRM

Table 3
Calibration curves, LODs and LOQs of the 10 analytes.

Analyte	Regression equation	R^2	Linear range (μg/mL)	LOD (μg/mL)	LOQ (μg/mL)
Histidine	$Y = 2.03 \times 10^6X + 6.65 \times 10^5$	0.9946	0.317–10.2	1.20×10^{-3}	1.95×10^{-2}
Aspartic acid	$Y = 7.13 \times 10^5X + 5.51 \times 10^4$	0.9990	0.256–16.4	3.13×10^{-2}	6.25×10^{-2}
Glutamic acid	$Y = 8.62 \times 10^5X + 4.25 \times 10^5$	0.9976	0.619–19.8	9.80×10^{-3}	7.81×10^{-2}
N-(*N*-glucopyranosyl)-indoleacetylaspartate	$Y = 2.57 \times 10^5X + 1.65 \times 10^5$	0.9990	0.313–99.9	9.80×10^{-3}	3.91×10^{-2}
N-(*N*-glucopyranosyl)-indoleacetylglutamate	$Y = 1.59 \times 10^5X - 7.00 \times 10^3$	0.9997	0.313–40.1	4.90×10^{-3}	9.80×10^{-3}
Eucomic acid	$Y = 1.46 \times 10^6X - 3.22 \times 10^5$	0.9992	0.311–19.9	2.40×10^{-3}	1.95×10^{-2}
Ginkgolide J	$Y = 5.64 \times 10^6X - 1.07 \times 10^5$	0.9996	9.66×10^{-2}–1.55	2.34×10^{-2}	4.69×10^{-2}
Ginkgolide C	$Y = 1.89 \times 10^6X + 2.94 \times 10^4$	0.9992	1.25×10^{-2}–0.400	2.44×10^{-4}	1.95×10^{-3}
Ginkgolide B	$Y = 1.01 \times 10^7X + 3.66 \times 10^6$	0.9933	2.61×10^{-2}–0.834	1.27×10^{-4}	5.09×10^{-4}
Ginkgolide A	$Y = 3.71 \times 10^4X + 4.29 \times 10^4$	0.9971	0.686–11.0	1.05×10^{-4}	8.37×10^{-4}

Table 4
Precision, repeatability, stability and recovery of the 10 analytes.

Analyte	Precision RSD (%)	Repeatability RSD (%)	Stability RSD (%)	Recovery (%)	Recovery RSD (%)
Histidine	2.93	4.43	4.07	104.74	4.03
Aspartic acid	1.35	4.3	2.96	88.84	3.21
Glutamic acid	1.72	2.8	3.60	102.61	2.23
N-(*N*-glucopyranosyl)-indoleacetylaspartate	1.97	2.79	2.46	97.29	3.79
N-(*N*-glucopyranosyl)-indoleacetylglutamate	3.29	2.97	3.07	97.99	2.25
Eucomic acid	2.83	1.90	1.49	97.62	2.61
Ginkgolide J	4.52	3.29	5.54	99.73	5.52
Ginkgolide C	3.82	3.49	5.37	98.00	3.27
Ginkgolide B	2.2	4.46	2.60	96.84	4.02
Ginkgolide A	2.39	2.13	2.37	96.01	5.24

chromatograms are shown in Fig. 8 (A for the standard solution and B for the test solution). A large variation in contents was observed for 10 analytes in 10 batches, as shown in Table 5. *N*-(*N*-glucopyranosyl)-indoleacetylaspartate was richest in each batch with the amount within 17.3–25.7 mg/g, while ginkgolide B (0.0270–0.0794 mg/g), ginkgolide C (0.0654–0.107 mg/g), ginkgolide J (0.0197–0.0335 mg/g), and histidine (0.177–0.382 mg/g) were determined to have the lowest amounts, below 1 mg/g. On the other hand, the contents of another 5 components generally ranged between 1 mg/g and 10 mg/g in 10 batches of GSDG, including *N*-(*N*-glucopyranosyl)-indoleacetylglutamate (3.54–5.31 mg/g), eucomic acid (3.36–5.51 mg/g), ginkgolide A (0.904–2.39 mg/g), aspartic acid (0.957–1.82 mg/g), and glutamic acid (1.22–2.81 mg/g). The relative contents for individual analytes in each batch were calculated using the average content of 10 batches as the denominator, and used for analysis of dispersion degree. As shown in Supplementary Table and Supplementary Fig. 6, all data were found to fall between 50 % and 150 % and the largest difference in content was seen for ginkgolide B (2.94-fold) among the different batches, while the least for *N*-(*N*-glucopyranosyl)-indoleacetylaspartate (1.49-fold). These results revealed the relative stable quality of these 10 batches of GSDG in terms of 10 chemical markers evaluated.

4. Conclusion

As a novel kind of Chinese medicine, DG has drawn significant concerns on its pharmacological and clinical researches, due to its similarity to traditional decoction. However, few studies on its chemical composition have been carried out.

To our knowledge, the present study is the first to reveal GSDG's chemical profiling by HPLC-QTOF-MS. With the observed accurate molecular masses, proposed fragmentation pathways, published literature, comparison with reference standards, as well as a home-made database and some on-line databases, 56 natural products have been identified or temporarily speculated, including 12 amino acids, 9 organic acids, 6 nucleosides and nucleobases, 6 flavonoids, 5 vitamins, 5 terpenoid lactones, 4 carbohydrates and 9 other components. Based on these results, an assay method was established for simultaneous determination of 10 representative bioactive components by HPLC-QTRAP-MS, by which the quality of 10 batches of GSDG was successfully evaluated. The validation in terms of linearity, stability, repeatability, precision and recovery has proven this assay method to be rapid, accurate, sensitive and convenient to operate. These mentioned methods may offer powerful support for the in-depth researches on GSDG in the future, especially in the fields of pharmaceutics, quality evaluation, pharmacokinetics, pharmacodynamic material basis and corresponding action mechanism. The present study can increase the knowledge and understanding of this Chinese medicine, and help utilize and develop it efficiently.

Ethics approval and consent to participate

Not applicable.

Consent for publication

Not applicable.

Funding

Not applicable.

Data availability statement

Data will be made available on request.

CRediT authorship contribution statement

Facheng Zhang: Writing – original draft, Conceptualization. **Qingqing Fei:** Writing – original draft, Investigation. **Xiaojun**

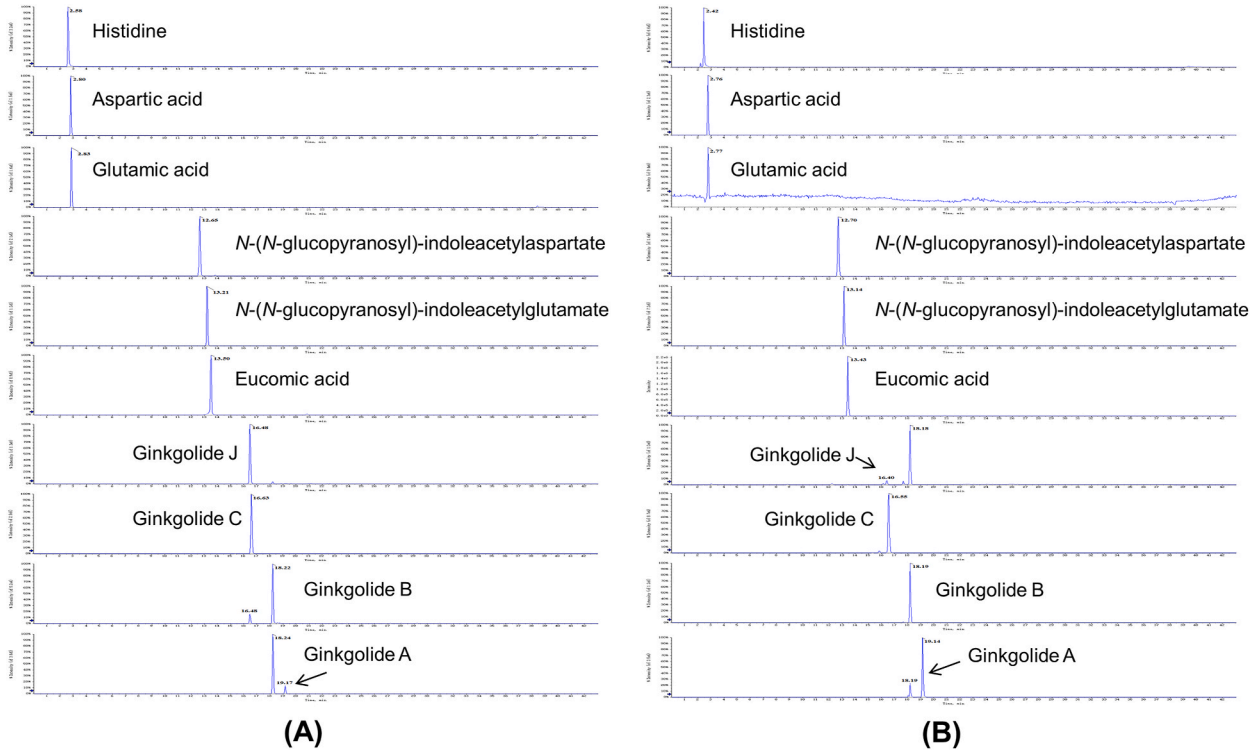

Fig. 8. MRM chromatograms of standard solution (A) and test solution (B).

Table 5
Contents of the 10 analytes in GSDG (mg/g).

Analyte	S1	S2	S3	S4	S5	S6	S7	S8	S9	S10	X ± SD
Histidine	0.382	0.290	0.296	0.177	0.244	0.325	0.284	0.261	0.186	0.343	0.279 ± 0.0649
Aspartic acid	1.04	0.957	1.63	1.66	1.82	1.75	1.81	1.49	1.09	1.23	1.45 ± 0.337
Glutamic acid	2.32	1.85	2.65	1.74	2.43	1.66	2.81	1.37	1.22	1.50	1.96 ± 0.558
N-(*N*-glucopyranosyl)-indoleacetylaspartate	25.2	17.3	19.0	20.4	25.7	22.8	18.9	23.0	21.1	22.2	21.6 ± 2.74
N-(*N*-glucopyranosyl)-indoleacetylglutamate	4.26	3.83	3.54	4.04	5.31	5.15	3.56	4.74	3.78	4.36	4.26 ± 0.633
Eucomic acid	5.51	3.58	4.80	5.06	3.36	5.17	4.92	4.30	4.22	3.99	4.49 ± 0.713
Ginkgolide J	0.0300	0.0238	0.0204	0.0335	0.0197	0.0318	0.0206	0.0295	0.0200	0.0254	0.0255 ± 0.00534
Ginkgolide C	0.0709	0.0984	0.0824	0.0683	0.0654	0.107	0.0782	0.0932	0.0724	0.0858	0.0822 ± 0.0139
Ginkgolide B	0.0576	0.0621	0.0794	0.0270	0.0392	0.0704	0.0726	0.0468	0.0298	0.0577	0.0543 ± 0.0181
Ginkgolide A	2.39	1.18	1.49	1.89	0.904	2.06	1.71	1.57	1.17	2.22	1.66 ± 0.488

Huang: Resources. **Sheng Yu:** Project administration, Investigation. **Rongli Qiu:** Resources. **Lan Guan:** Supervision. **Baoxiang Wu:** Investigation, Conceptualization. **Mingqiu Shan:** Writing – review & editing, Supervision, Conceptualization.

Declaration of competing interest

The authors declare that they have no known competing financial interests or personal relationships that could have appeared to influence the work reported in this paper.

Acknowledgements

Not applicable.

Appendix A. Supplementary data

Supplementary data to this article can be found online at https://doi.org/10.1016/j.heliyon.2024.e36909.

References

[1] R.J. Qiu, X.Y. Zhang, C. Zhao, M. Li, H.C. Shang, Comparison of the efficacy of dispensing granules with traditional decoction: a systematic review and meta-analysis, Ann. Transl. Med. 6 (2018) 38.
[2] L.L. Qin, M. Yu, H.X. Zhang, H.M. Jia, X.C. Ye, Z.M. Zou, Quality markers of Baizhu dispensing granules based on multi-component qualitative and quantitative analysis combined with network pharmacology and chemometric analysis, J. Ethnopharmacol. 288 (2022) 114968.
[3] C.Y. Zhang, X.X. Li, P. Li, Y. Jiang, H.J. Li, Consistency evaluation between dispensing granule and traditional decoction from Coptidis Rhizoma by using an integrated quality-based strategy, Phytochem. Anal. 32 (2021) 153–164.
[4] E.X. Shang, Z.H. Zhu, L. Liu, Y.P. Tang, J.A. Duan, UPLC-QTOF-MS with chemical profiling approach for rapidly evaluating chemical consistency between traditional and dispensing granule decoctions of Tao-Hong-Si-Wu decoction, Chem. Cent. J. 6 (2012) 143.
[5] H. Zhou, C.Z. Wang, J.Z. Ye, H.X. Chen, R. Tao, F.L. Cao, Effects of high hydrostatic pressure treatment on structural, allergenicity, and functional properties of proteins from ginkgo seeds, Innov. Food Sci. Emerg. 34 (2016) 187–195.
[6] Y.X. Liu, H.W. Xin, Y.C. Zhang, F.Y. Che, N. Shen, Y.L. Cui, Leaves, seeds and exocarp of Ginkgo biloba L. (Ginkgoaceae): a Comprehensive Review of Traditional Uses, phytochemistry, pharmacology, resource utilization and toxicity, J. Ethnopharmacol. 298 (2022) 115645.
[7] N. Mei, X.Q. Guo, Z. Ren, D. Kobayashi, K. Wada, L. Guo, Review of *Ginkgo biloba*-induced toxicity, from experimental studies to human case reports, J. Environ. Sci. Health C Environ. Carcinog. Ecotoxicol. Rev. 35 (2017) 1–28.
[8] Y. Feodorova, T. Tomova, D. Minchev, V. Turiyski, M. Draganov, M. Argirova, Cytotoxic effect of *Ginkgo biloba* kernel extract on HCT116 and A2058 cancer cell lines, Heliyon 6 (2020) e04941.
[9] Y.Y. Qian, L. Yan, M. Wei, P.P. Song, L.H. Wang, Seeds of Ginkgo biloba L. inhibit oxidative stress and inflammation induced by cigarette smoke in COPD rats through the Nrf2 pathway, J. Ethnopharmacol. 301 (2023) 115758.
[10] Q. Zhang, C.N. Tan, L. Cai, F.B. Xia, D. Gao, F.Q. Yang, H. Chen, Z.N. Xia, Characterization of active antiplatelet chemical compositions of edible *Citrus limon* through ultraperformance liquid chromatography single quadrupole mass spectrometry-based chemometrics, Food Funct. 9 (2018) 2762–2773.
[11] Q.D. Liu, C.Y. Xie, L.L. Yan, X.J. Xu, D.P. Yang, High performance liquid chromatography-DAD-mass spectrometry analysis of Citri grandis exocarpium, Mod. Tradit. Chin. Med. Materia Medica-World Sci. Technol. 13 (2011) 864–867.
[12] Y.M. Zhao, S.X. Liu, C.X. Zhang, D.L. Liu, T.J. Zhang, Analysis on chemical constituents from Glycyrrhizae Radix et Rhizoma by HPLC-Q-TOF-MS, Chin. Tradit. Herbal Drugs 47 (2016) 2061–2068.
[13] L. Konieczna, M. Pyszka, M. Okońska, M. Niedźwiecki, T. Bączek, Bioanalysis of underivatized amino acids in non-invasive exhaled breath condensate samples using liquid chromatography coupled with tandem mass spectrometry, J. Chromatogr. A 1542 (2018) 72–81.
[14] Y.M. She, X.H. Xiong, Y. Zhou, S.Y. Liu, Characteristic fragmentations of [MH-CO2H2]+ in two kinds of amino acid, Acta Phys. Chim. Sin. 13 (1997) 252–257.
[15] N. Xu, Z.Q. Zhu, S.P. Yang, J. Wang, H.W. Gu, Z. Zhou, H.W. Chen, Direct detection of amino acids using extractive electrospray ionization tandem mass spectrometry, Chin. J. Anal. Chem. 41 (2013) 523–528.
[16] Y.Y. Fu, M.Q. Shan, M.H. Hu, Y.L. Jiang, P.D. Chen, Y.M. Chi, S. Yu, L. Zhang, Q.N. Wu, F.C. Zhang, Z.Y. Mao, Chemical profiling of Banxia-Baizhu-Tianma decoction by ultra-fast liquid chromatography with tandem mass spectrometry, J. Pharmaceut. Biomed. 174 (2019) 595–607.
[17] J.X. Zhou, S. Yu, B.Q. Wang, X. Wei, L. Zhang, M.Q. Shan, Chemical profiling and quantification of Yihuang decoction by high performance liquid chromatography coupled with quadrupole time-of-flight mass spectrometry and a diode array detector, J. Pharmaceut. Biomed. 224 (2023) 115199.
[18] C. Simmler, C. Antheaume, P. André, F. Bonté, A. Lobstein, Glucosyloxybenzyl eucomate derivatives from vanda teres stimulate HaCaT cytochrome c oxidase, J. Nat. Prod. 74 (2011) 949–955.
[19] A. Mata, J.P. Ferreira, C. Semedo, T. Serra, C.M.M. Duarte, M.R. Bronze, Contribution to the characterization of Opuntia spp. juices by LC-DAD-ESI-MS/MS, Food Chem. 210 (2016) 558–565.
[20] R. Capilla-Flores, G. Egea-Castro, R. López-Ruíz, R. Romero-González, A.G. Frenich, Development of novel methods based on GC-HRMS and LC-HRMS for the determination of non-phthalate plasticizers in soil, Sci. Total Environ. 917 (2024) 170150.
[21] R. Preuss, H.M. Koch, J. Angerer, Biological monitoring of the five major metabolites of di-(2-ethylhexyl)phthalate (DEHP) in human urine using column-switching liquid chromatography–tandem mass spectrometry, J. Chromatogr. B 816 (2005) 269–280.
[22] N.E. Thomford, K. Dzobo, F. Adu, S. Chirikure, A. Wonkam, C. Dandara, Bush mint (Hyptis suaveolens) and spreading hogweed (Boerhavia diffusa) medicinal plant extracts differentially affect activities of CYP1A2, CYP2D6 and CYP3A4 enzymes, J. Ethnopharmacol. 211 (2018) 58–69.
[23] R. Jaiswal, E.A. Halabi, M.G.E. Karar, N. Kuhnert, Identification and characterisation of the phenolics of *Ilex glabra* L. Gray (Aquifoliaceae) leaves by liquid chromatography tandem mass spectrometry, Phytochemistry 106 (2014) 141–155.
[24] N.B. Fang, S.G. Yu, R.L. Prior, LC/MS/MS characterization of phenolic constituents in dried plums, J. Agric. Food Chem. 50 (2002) 3579–3585.
[25] Z.H. Wang, X.L. Li, S.J. Zhen, X.Y. Li, C.W. Wang, Y.J. Wang, The important role of quinic acid in the formation of phenolic compounds from pyrolysis of chlorogenic acid, J. Therm. Anal. Calorim. 114 (2013) 1231–1238.
[26] Q.F. Zhang, Y.X. Guo, G.D. Zheng, W.J. Wang, Chemical constituents comparison between Rhizoma Smilacis Glabrae and Rhizoma Smilacis Chinae by HPLC-DAD-MS/MS, Nat. Prod. Res. 27 (2013) 277–281.
[27] Y.N. Gai, H. Chen, C.Y. Wu, F. Feng, Y.X. Wang, W.Y. Liu, S.L. Wang, Analysis of the traditional medicine YiGan San by the fragmentation patterns of cadambine indole alkaloids using HPLC coupled with high-resolution MS, J. Sep. Sci. 36 (2013) 3723–3732.
[28] B. Kammerer, A. Frickenschmidt, C.E. Müller, S. Laufer, C.H. Gleiter, H. Liebich, Mass spectrometric identification of modified urinary nucleosides used as potential biomedical markers by LC-ITMS coupling, Anal. Bioanal. Chem. 382 (2005) 1017–1026.
[29] N.P. Vedenicheva, G.A. Al-Maali, N.A. Bisko, M.M. Shcherbatiuk, M.L. Lomberg, N.Y. Mytropolska, O.B. Mykchaylova, I.V. Kosakivska, Comparative analysis of cytokinins in mycelial biomass of medicinal mushrooms, Int. J. Med. Mushrooms 20 (2018) 837–847.
[30] Z.H. Li, H. Guo, W.B. Xu, J. Ge, X. Li, M. Alimu, D.J. He, Rapid identification of flavonoid constituents directly from PTP1B inhibitive extract of raspberry (*Rubus idaeus* L.) leaves by HPLC–ESI–QTOF–MS-MS, J. Chromatogr. Sci. 54 (2016) 805–810.
[31] R.M. Ibrahim, A.M. El-Halawany, D.O. Saleh, E. El Naggar, A.O. El-Shabrawy, S.S. El-Hawary, HPLC-DAD-MS/MS profiling of phenolics from Securigera securidaca flowers and its anti-hyperglycemic and anti-hyperlipidemic activities, Rev. Bras. Farmacogn. 25 (2015) 134–141.
[32] Z. Ouyang, X. Cao, Y. Wei, W.W.Q. Zhang, M. Zhao, J.A. Duan, Pharmacokinetic study of rutin and quercetin in rats after oral administration of total flavones of mulberry leaf extract, Rev. Bras. Farmacogn. 23 (2013) 776–782.
[33] J. Yang, D.W. Qian, S. Jiang, E.X. Shang, J.M. Guo, J.A. Duan, Identification of rutin deglycosylated metabolites produced by human intestinal bacteria using UPLC–Q-TOF/MS, J. Chromatogr. B 898 (2012) 95–100.
[34] M.A. Astiti, A. Jittmittraphap, P. Leaungwutiwong, N. Chutiwitoonchai, P. Pripdeevech, C. Mahidol, S. Ruchirawat, P. Kittakoop, LC-QTOF-MS/MS based molecular networking approach for the isolation of α-glucosidase inhibitors and virucidal agents from *Coccinia grandis* (L.) voigt, Foods 10 (2021) 3041.
[35] G. Abdel-Moez, B. Avula, H. Sayed, A. Khalifa, S. Ross, K. Katragunta, I. Khan, S. Mohamed, Phytochemical profiling of three *Amaranthus* species using LC-MS/MS metabolomic approach and chemometric tools, J. Pharmaceut. Biomed. 236 (2023) 115722.

[36] S. Saha, P.A. Kroon, A simple and rapid LC-MS/MS method for quantification of total daidzein, genistein, and equol in human urine, J. Anal. Methods Chem. 2020 (2020) 2359397.
[37] A. Girme, P. Bhoj, G. Saste, S. Pawar, A. Mirgal, D. Raut, M. Chavan, L. Hingorani, Development and validation of RP-HPLC method for vicenin-2, orientin, cynaroside, betulinic acid, genistein, and major eight bioactive constituents with LC-ESI-MS/MS profiling in *ocimum* genus, J. AOAC Int. 104 (2021) 1634–1651.
[38] M. Siniawska, A. Wojdyło, Polyphenol profiling by LC QTOF/ESI-MS and biological activity of purple passion fruit epicarp extract, Molecules 28 (2023) 6711.
[39] M. Khaksari, L.R. Mazzoleni, C.H. Ruan, R.T. Kennedy, A.R. Minerick, Data representing two separate LC-MS methods for detection and quantification of water-soluble and fat-soluble vitamins in tears and blood serum, Data Brief 11 (2017) 316–330.
[40] A. Aslam, S.J. Zhao, X.Q. Lu, N. He, H.J. Zhu, A.U. Malik, M. Azam, W.G. Liu, High-throughput LC-ESI-MS/MS metabolomics approach reveals regulation of metabolites related to diverse functions in mature fruit of grafted watermelon, Biomolecules 11 (2021) 628.
[41] S.M. Sallabi, A. Alhmoudi, M. Alshekaili, I. Shah, Determination of vitamin B3 vitamer (nicotinamide) and vitamin B6 vitamers in human hair using LC-MS/MS, Molecules 26 (2021) 4487.
[42] A. Maus, A. Girtman, J. Kiesling, J. Faber, S.K.G. Grebe, Overcoming the chromatographic challenges when performing LC-MS/MS measurements of pyridoxal-5′-phosphate, J. Chromatogr. B 1217 (2023) 123605.
[43] S. Ghassabian, L. Griffiths, M.T. Smith, A novel fully validated LC–MS/MS method for quantification of pyridoxal-5′-phosphate concentrations in samples of human whole blood, J. Chromatogr. B 1000 (2015) 77–83.
[44] C.M. Geng, X. Guo, J.J. Liu, G.Y. Yuan, F.L. Bu, X.W. Chen, B.J. Wang, R.C. Guo, LC–MS/MS for the determination of four water-soluble vitamins: method development, validation and comparison to EC method, Chromatographia 80 (2017) 259–264.
[45] J.C. Li, D.P. Li, J.H. Hu, Y. Bi, W. Xiao, Z.Z. Zhang, Simultaneous determination of ginkgolides A, B, C and bilobalide by LC-MS/MS and its application to a pharmacokinetic study in rats, Biomed. Chromatogr. 29 (2015) 1907–1912.
[46] J.Y. Qiu, X. Chen, Z. Li, S.R. Wang, X.W. Wu, Y.J. Li, D.Z. Yang, Y.Y. Yu, X.X. Yin, D.Q. Tang, LC–MS/MS method for the simultaneous quantification of 11 compounds of *Ginkgo biloba* extract in lysates of mesangial cell cultured by high glucose, J. Chromatogr. B 997 (2015) 122–128.
[47] T.P. Dew, G. Wang, G. Williamson, Urinary excretion of ginkgolide terpene lactones following acute consumption of *Ginkgo biloba* extract, Biofactors 40 (2014) 268–274.
[48] L.T. Wang, H. Huang, Y.H. Chang, Y.Q. Wang, J.D. Wang, Z.H. Cai, T. Efferth, Y.J. Fu, Biflavonoids from *Ginkgo biloba* leaves as a novel anti-atherosclerotic candidate: inhibition potency and mechanistic analysis, Phytomedicine 102 (2022) 154053.
[49] B. Avula, Y.H. Wang, T.J. Smillie, I.A. Khan, Column liquid chromatography/electrospray ionization-time of flight-mass spectrometry and ultraperformance column liquid chromatography/mass spectrometry methods for the determination of ginkgolides and bilobalide in the leaves of *Ginkgo biloba* and dietary supplements, J. AOAC Int. 92 (2009) 645–652.
[50] K. Woelkart, E. Feizlmayr, P. Dittrich, E. Beubler, F. Pinl, A. Suter, R. Bauer, Pharmacokinetics of bilobalide, ginkgolide A and B after administration of three different *Ginkgo biloba* L. Preparations in humans, Phytother Res. 24 (2010) 445–450.
[51] M.J. Huddleston, M.F. Bean, S.A. Carr, Collisional fragmentation of glycopeptides by electrospray ionization LC/MS and LC/MS/MS: methods for selective detection of glycopeptides in protein digests, Anal. Chem. 65 (1993) 877–884.
[52] Y.L. Huang, B.Y. Jhou, S.F. Chen, K.H. Khoo, Identifying specific and differentially linked glycosyl residues in mammalian glycans by targeted LC-MS analysis, Anal. Sci. 34 (2018) 1049–1054.
[53] P. Lijina, J.R. Manjunatha, B.S.G. Kumar, Characterization of free oligosaccharides from garden cress seed aqueous exudate using PGC LC-MS/MS and NMR spectroscopy, Carbohydr. Res. 532 (2023) 108914.
[54] S. Agrawal, A.C. Bisen, A. Biswas, S.N. Sanap, S.K. Verma, M. Kumar, S. Jaiswal, A. Kumar, T. Narender, S. Bhatta, Simultaneous pharmacokinetic assessment of phytopharmaceuticals in fenugreek extract using LC–MS/MS in Sprague–Dawley rats, Biomed. Chromatogr. 37 (2023) e5600.
[55] B. Noorani, E.A. Chowdhury, F. Alqahtani, Y. Ahn, D. Patel, A. Al-Ahmad, R. Mehvar, U. Bickel, LC-MS/MS-based in vitro and in vivo investigation of blood-brain barrier integrity by simultaneous quantitation of mannitol and sucrose, Fluids Barriers CNS 17 (2020) 61.
[56] J.T. Cheng, C. Guo, W.J. Cui, Q. Zhang, S.H. Wang, Q.H. Zhao, D.W. Liu, J. Zhang, S. Chen, C. Chen, Y. Liu, Z.H. Pan, A. Liu, Isolation of two rare N-glycosides from *Ginkgo biloba* and their anti-inflammatory activities, Sci. Rep. 10 (2020) 5994.
[57] P.M. Scott, B.P. Lau, G.A. Lawrence, D.A. Lewis, Analysis of *Ginkgo biloba* for the presence of ginkgotoxin and ginkgotoxin 5′-glucoside, J. AOAC Int. 83 (2000) 1313–1320.
[58] A.S. Abouzied, M.M. Abd-Rabo, B. Huwaimel, S.A. Almahmoud, A.A. Almarshdi, F.M. Alharbi, S.S. Alenzi, B.N. Albsher, A. Alafnan, In silico pharmacokinetic profiling of the identified bioactive metabolites of pergularia tomentosa L. Latex extract and in vitro cytotoxic activity via the induction of caspase-dependent apoptosis with S-phase arrest, Pharmaceuticals 15 (2022) 1132.
[59] R. Zhang, C.R. Zhao, X.W. Gong, J. Yang, G.F. Zhang, W. Zhang, Ginkgolide C alleviates acute lung injury caused by paraquat poisoning via regulating the Nrf2 and NF- κ B signaling pathways, Oxid. Med. Cell. Longev. 2022 (2022) 7832983.
[60] M.H. Yang, I.J. Ha, S.G. Lee, J.Y. Um, K.S. Ahn, Abrogation of STAT3 activation cascade by Ginkgolide C mitigates tumourigenesis in lung cancer preclinical model, J. Pharm. Pharmacol. 73 (2021) 1630–1642.
[61] Y.J. Xiang, S.Y. Zhang, J. Lu, W. Zhang, M. Cai, J. Xiang, D.F. Cai, Ginkgolide B protects human pulmonary alveolar epithelial A549 cells from lipopolysaccharide-induced inflammatory responses by reducing TRIM37-mediated NF-κB activation, Biotechnol. Appl. Biochem. 67 (2020) 903–911.
[62] A.L. Wang, J. Wan, F. Xu, Ginkgolide A reduces airway inflammation in a neutrophil-predominant murine model of asthma via suppression of immune response of helper T cell 17, Chin. J. Integr. Tradit. West. Med. Intens. Crit. Care 26 (2019) 564–568.
[63] Q.S. Tian, M. Xu, B. He, Histidine ameliorates elastase- and lipopolysaccharide-induced lung inflammation by inhibiting the activation of the NLRP3 inflammasome, Acta Biochim. Biophys. Sin. 53 (2021) 1055–1064.
[64] N. Salyha, Y. Salyha, L-Glutamic acid mitigates carbon tetrachloride-induced acute tissue injury by reducing oxidative stress in a rat model, Curr. Chem. Biol. 16 (2022) 130–137.
[65] Q. Zhang, Q. Wang, J.T. Cheng, S. Chen, A. Liu, Y.S. Wang, The bioavailability and excretion of an antitussive compound IAsp-N-Glc in rats by validated UPLC-MS/MS methods, Pak. J. Pharm. Sci. 33 (2020) 1403–1411.
[66] H. Khan, Marya, T. Belwal, M. Tariq, A.G. Atanasov, H.P. Devkota, Genus *Vanda*: a review on traditional uses, bioactive chemical constituents and pharmacological activities, J. Ethnopharmacol. 229 (2019) 46–53.